Critical Issues of Current Research on the Dynamics Leading to Glass Transition†

S. Capaccioli

Dipartimento di Fisica, Università di Pisa and CNR-INFM, polylab, Largo Bruno Pontecorvo, 3, I-56127 Pisa, Italy

M. Shahin Thayyil

Dipartimento di Fisica, Università di Pisa, Largo Bruno Pontecorvo, 3, I-56127 Pisa, Italy, and Department of Physics, University of Calicut, Kerala, India

K. L. Ngai*

Naval Research Laboratory, Washington, DC 20375-5320

Received: June 30, 2008; Revised Manuscript Received: August 25, 2008

Glass transition is still an unsolved problem in condensed matter physics and chemistry. In this paper, we critically reexamine experimental data and theoretical interpretations of dynamic properties of various processes seen over a wide time range from picoseconds to laboratory time scales. In order of increasing time, the ubiquitous processes considered include (i) the dynamics of caged molecular units with motion confined within the anharmonic intermolecular potential and where no genuine relaxation has yet taken place; (ii) the onset of the Johari−Goldstein secondary relaxation involving rotation or translation of the entire molecular unit and causing the decay of the cages, to be followed by the cooperative and dynamically heterogeneous motions participated by increasing number of molecules or length scale; and (iii) the terminal primary α-relaxation with the maximum cooperative length-scale allowed by the intermolecular interaction and constraints of the glass former. Some general and important properties found in each of these processes are shown to be interrelated, indicating that the processes are connected, with one being the precursor of the other following it. Thus, a theory of glass transition is neither complete nor fundamental unless all of these processes and their inter-relations have been accounted. In addition to published data, new experimental data are reported here to provide a limited collection of critical experimental facts having an impact on current issues of glass transition research and serving as a guide for the construction of a complete and successful theory in the future.

1. Introduction

Although research in glass-forming substances and the glass transition problem has a long history, considerable advances have been made in the last two decades on both the experimental and the theoretical fronts. The dynamic properties of many different glass formers are now known over immensely wide frequency ranges from vibration frequencies down to as low as 10^{-6} Hz in some cases. Investigations by various experimental techniques have established a host of general facts on the dynamics over such wide frequency/time ranges. It is challenging to interpret or explain in full by theory this vast amount of experimental facts. Often, a subset of the experimental findings and a restricted class of glass formers can be satisfactorily explained by some theory. However, if the interpretation or explanation is inconsistent with other experimental results outside the subset, the theory is untenable and no real progress in the field has been made. This unfortunate situation can easily happen to any theoretical attempt because of the exceedingly large number of nontrivial and often general dynamic properties that have been established over wide frequency/time ranges. This pitfall can be avoided if all critical and essential experimental results are collectively considered, or at least borne in mind, when interpreting any specific experimental data. By no means can this be easily done, but it is absolutely necessary; for otherwise, one cannot be sure whether or not the theory is sufficient or already has contradicted some other experimental facts not considered. For this reason, we examine in this paper the general and critical experimental results of several characteristic dynamic processes of glass formers that have been seen over 18 decades of time, from picoseconds to days. Recognition of all of these general properties is vital for correct and complete interpretations and for the construction of a fully satisfactory theory in the future.

The paper is a critical reexamination of experimental data and theoretical interpretations of dynamics seen over several different time scales and how they are related to each other. In the order of increasing time, these different dynamics include the motion of molecular units when caged or confined within the anharmonic intermolecular potential and no genuine relaxation has yet to occur (the caged regime), the onset of the local and independent relaxation (i.e., the conventional secondary relaxation) and concomitant decay of the cages, the cooperative and dynamically heterogeneous motion that participated by an increasing number of molecules, and finally the terminal primary α-relaxation with the maximum cooperative length scale allowed by the intermolecular interaction and constraints of the glass former. In addition to published data, new experimental data are reported here to provide a

† Part of the "Karl Freed Festschrift".

10.1021/jp8057433 CCC: $40.75 © 2008 American Chemical Society
Published on Web 10/17/2008

collection of critical experimental facts with which any viable theory must be consistent. From these experimental facts, we make our own judgment on current issues of research in the field of glass transition. We encourage the readers to make their own judgments from the same experimental facts presented here. Either way is deemed to be beneficial to promote advancement in the research field of glass transition.

2. Experimental Section

In addition to the data already published and critically reanalyzed here, experimental data on new systems are presented. Samples used in the experiments are benzophenone (BZP, $T_g = 207$ K) and diisobutylphthalate (DiBP, $T_g = 188$ K), which were obtained from Sigma-Aldrich and used as received. Polystyrene 800 (PS800) with a molecular weight = 820 g mol^{-1}, $M_w/M_n = 1.01$, and $T_g = 282$ K was obtained from Scientific Polymer Products. All samples were stored and handled in a dry nitrogen atmosphere. The polar molecules were dissolved in PS800 in small molar concentrations (determined by mass balance).

Dielectric measurements were carried out using a Novocontrol Alpha-Analyzer ($10^{-2}-10^{7}$ Hz). The sample cell, made up by a parallel plate stainless steel capacitor separated by quartz spacers (geometric capacitance, ~100 pF), was filled with the sample and placed in the nitrogen flow. A Quatro cryostat was used for temperature control in the range of 90−400 K. The samples were cooled much below the glass transition temperature, and dielectric spectra were measured isothermally at higher temperatures during heating, after stabilizing the temperature within 0.1 K for about 30 min. For measurements in the glass transition region, the temperature was stabilized for about 60 min.

3. Fast Processes

Fast dynamics observed by experiments and molecular dynamics (MD) simulations are most often discussed in the context of the various versions of the mode coupling theory (MCT).[1−11] The data were commonly used to show consistency with the predictions of MCT and, sometimes, the deviation or inadequacy. This special attention paid to MCT is natural because MCT is a mathematically rigorous theory that tries to explain the fast processes in the short time regime when all molecules are mutually caged. However, this fixation toward one theory has the downside of neglecting other possible interpretations, which may offer better collective explanation of the experimental data and resolution of the problem. Despite the idealized or schematic MCT that had been favorably compared with experiments and MD simulations of fast processes in many glass formers (often the "fragile" ones but not the "strong" ones such as $ZnCl_2$[12] and B_2O_3[13]), some new experiments have shown features of the fast processes in "fragile" glass formers that cannot be explained. The first came in 2000 from optical heterodyne detected optical Kerr effect (OHD-OKE) experiments on salol (phenyl salicylate).[14] The entire data extending from 2 up to about 3×10^4 ps were well-fitted by the function

$$S(t) = [pt^{-1+c} + dt^{-1+b}]\exp(-t/\tau_\alpha) \qquad (1)$$

In a range of time longer than 2 ps and extending to some longer times that increase with decreasing temperature, a portion of the OHD-OKE signal, $S(t)$, exhibits a power law decay pt^{-1+c} (the first term inside the bracket in eq 1). Here, p is the amplitude, and the positive fractional exponent c has significant temperature dependence and decreases to a value close to 0 at temperatures somewhat below the critical temperature T_c of MCT. Because this new feature appears on time scales longer than intramolecular vibrations and before the von Schweidler power law of MCT (the second term inside the bracket in eq 1), it is called the intermediate power law (IPL).[14] The IPL with $c \approx 0$ is not predicted by the idealized MCT.[3,4] The extended MCT[6−8] that introduces, in addition, a full range of hopping times also cannot explain the IPL and its temperature dependence near and below T_c. If c were exactly zero, then the IPL would correspond to the logarithmic time dependence of the polarization−polarization correlation function. Perhaps it is for this reason that the OHD-OKE data were sometimes referred to as logarithmic decay of the orientational correlation function.[9,15] Logarithmic decay of correlation function was found also by photon correlation spectroscopy in dense colloidal suspensions.[16] The existence of the IPL with exponent $c \approx 0$ or equivalently the logarithmic decay was well-recognized by Götze and Sperl.[9] In 2002, a special solution of MCT for states near higher order glass transition singularities that has a correlation function with logarithmic decay was proposed by them to explain the OHD-OKE data.[9]

The OHD-OKE signal $S(t)$ measures the time derivative of the polarizability−polarizability correlation function,[17] which is equivalent to the time derivative of the orientational correlation function $\phi(t)$ of the molecules. Therefore, the Fourier transform of $S(t)$ to the frequency domain is the susceptibility spectrum $\chi''(\nu)$ that can be obtained directly by dynamic light scattering experiment.[8,18,19] In particular, the time dependence t^{-1+c} of the IPL corresponds to the frequency dependence ν^{-c} of $\chi''(\nu)$. Because c becomes small at lower temperatures, the t^{-1+c} decay of $S(t)$ corresponds to ν^{-c} of $\chi''(\nu)$ with $c \ll 1$, which is appropriately called the nearly constant loss (NCL) in the susceptibility $\chi''(\nu)$ or the dielectric loss $\varepsilon''(\nu)$ spectrum. Immediately following the OHD-OKE experiment on salol[14] is the publication of $\chi''(\nu)$ data of polyisobutylene (PIB) in the $5 < \nu < 40$ GHz range from dynamic light scattering experiments.[18] This publication[18] reported the observation of susceptibility spectra that have the power law dependence, $\chi''(\nu) = p'\nu^{-c}$ with $c \ll 1$, an exact correspondent of the IPL, pt^{-1+c} with $c \ll 1$. The measured $\chi''(\nu)$ of PIB is nearly frequency independent over a broad temperature range from below T_g to higher than $1.3T_g$. The same was found in another polymer, 1,4-polyisoprene (PI).[20] The temperature dependence of the amplitude p' is weak, approximately linear, and increasing by about a factor of 4 from $T_g \approx 200$ K to nearly 290 K.[21] The temperature dependence of p of PIB and PI is weaker below T_g than above T_g and exhibits a change of slope at T_g.[21] The sensitivity of the NCL in these two polymers to glass transition is remarkable when considering that it was observed in the GHz range, corresponding to times of order of 10^{-10} s, whereas the glass transition at T_g occurs at a time scale of thousands of seconds. If NCL originates from excursions of caged molecules within anharmonic potential and fluctuations of cages, then a possible explanation can be considered as follows. The amplitudes of fluctuations and excursions depend on temperature through density and entropy. The change in the temperature dependences of density and entropy when crossing T_g is well-known, and this change leads to a corresponding change of the T dependence of amplitudes of fluctuations and excursions and, hence, the intensity of the NCL. No further change of the T dependence of p' was observed above T_g, up to temperatures as high as $1.3T_g$.

Similar observations of the presence of the NCL were made from dynamic light scattering data of glycerol and poly(methylmethacrylate) (PMMA).[22] It is worthwhile to point out that while dynamic light scattering can measure the NCL of glycerol in the $5 < \nu < 40$ GHz range at 160 (below T_g) and 200 K (above T_g), the best broadband dielectric relaxation measurement of glycerol by Lunkenheimer and co-workers[23] lacks the sensitivity to detect the low dielectric loss in the same frequency and temperature ranges. Consequently, no dielectric loss $\varepsilon''(\nu)$ data of glycerol were reported in the GHz to 40 GHz frequency range at temperatures below 213 K. The $\varepsilon''(\nu)$ data obtained[23] above 100 GHz and below 1 GHz at 195 K or below 10^{-1} GHz at 184 K (see Figure 4 in ref 23), for example, were interpolated by others[24] by a smooth curve to suggest the presence of a minimum (see Figure 1a in ref 24) instead of the NCL found directly in the dynamic light scattering data. Dielectric measurements in other glass formers that have no resolved secondary relaxation as glycerol suffer the same problem of not having the sensitivity to see the NCL in the same high-frequency region as in the case of glycerol. These include propylene carbonate (at $T = 163$ K, $T_g = 159$ K),[23] 2-picoline, propylene glycol, and 4-*tert*-butyl-pyridine.[25,26] Returning to the dielectric data of glycerol at 195 and 184 K,[23]the loss measured at frequencies lower than 10^{-1} GHz shows a power law decrease of $\varepsilon''(\nu) \sim \nu^{-c}$ with $c \approx 0.23$ and 0.17, respectively, in excess on the high-frequency side of the fit of the α-relaxation loss peak by either the Cole−Davidson empirical function or the one-sided Fourier transform of the Kohlrausch stretched exponential function. Similar excess loss, $\varepsilon''(\nu) \sim \nu^{-c}$ with $c \approx 0.2$ to 0.3 was found in the susceptibility spectrum of the other glass formers [23,25,26] and is often called the "excess wing", which corresponds in the time domain to the IPL, $\varepsilon(t)$ or $\chi(t) \sim t^{-1+c}$, with $c \approx 0.2-0.3$. Perhaps it is the inability of dielectric spectroscopy to reveal the presence of the NCL at high frequencies (>1 GHz) that has led others to emphasize exclusively the excess wing $c \approx 0.2$ or about as a fundamental feature of the dynamics at all temperatures,[19,24,27] but not the NCL, although it was actually seen by experiments. NCL was found by dynamic light scattering[18,20−22] as $\chi''(\nu) = p'\nu^{-c}$, and in OHD-OKE[14,15] as the IPL, t^{-1+c}, with c nearly zero in both cases. Even in the high-frequency range ($10^{-3} < \nu < 10^2$ GHz), the dielectric relaxation experiment has found the NCL in $0.4Ca(NO_3)_2-0.6KNO_3$ (CKN, $T_g = 335$ K) as $\varepsilon''(\nu) = p'\nu^{-c}$ with $c \approx 0$. This is made possible by the sizable dielectric loss higher than 0.1 of CKN at 342 K and higher temperatures[28] (at these temperatures, the structural α-relaxation and the ionic conductivity relaxation are coupled together[29]). Thus, from the experimental evidence given above, the NCL found at higher frequencies and temperatures is also an important and fundamental feature of the dynamics and should not be forgotten for the sake of emphasizing the excess wing in dielectric relaxation (at frequencies below 1 GHz) and dynamic light scattering or IPL in OHD-OKE all with $c \approx 0.2$ or about.[24,27] This is also clear from the fact that the NCL is needed to explain the flat susceptibility instead of a minimum at high frequencies from dynamic light scattering[18,20−22] and some IPL with c nearly zero from OHD-OKE.[14,15] Later on, we shall return to discuss the origin of this so-called excess wing and its relation to the NCL, which is actually the precursor of the excess wing.

The dielectric data discussed above are all at temperatures above T_g. When the temperature is lowered to below T_g, the exponent c of the excess wing, $\varepsilon''(\nu) \sim \nu^{-c}$, decreases monotonically to reach $c \approx 0.1$ or less and extends over many decades of frequency. This is perhaps first seen dielectrically

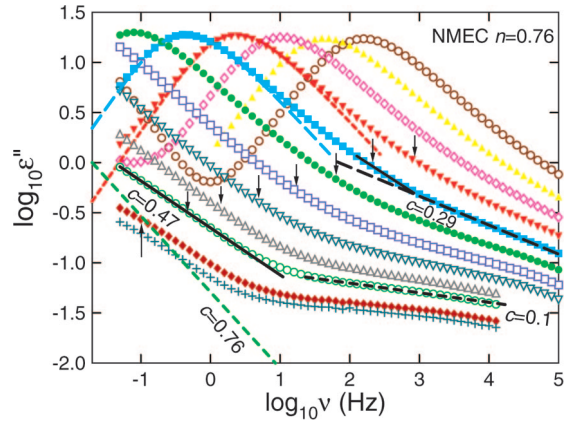

Figure 1. Dielectric loss spectra of NMEC at temperatures above and slightly below T_g (from right to left: 186, 184, 182, 180, 178, 176, 174, 172, 170, 168, 164, and 162 K) showing the following three distinct relaxation mechanisms. (i) The α-loss peaks and the fits (red and pale blue dashed lines) at two temperatures by the Fourier transform of the KWW function, $\phi(t) = \exp[-(t/\tau_\alpha)^{1-n}]$, with $n = 0.24$. (ii) The excess loss $\varepsilon''(\nu) \sim \nu^{-c}$ with $c = 0.29$ (long dashed line) at 178 K and with $c = 0.47$ (solid line) at 168 K. The very different slopes of the excess loss at the same levels at the two temperatures rule out frequency−temperature superposition of the loss data of the excess loss in this region. (ii) The emergence of the NCL, $\varepsilon''(\nu) \sim \nu^{-c}$ with $c \approx 0.1$ (black short dashed line), with lower intensity at lower temperatures. The green dashed line with the label $c \approx 0.76$ shows the frequency dependence of the high-frequency flank of the KWW fit to the (unobserved) loss peak at 168 K. The vertical arrows indicate the relaxation time of the unresolved Johari−Goldstein (JG) β-relaxation suggested by the coupling model (CM). For more details, see the text.

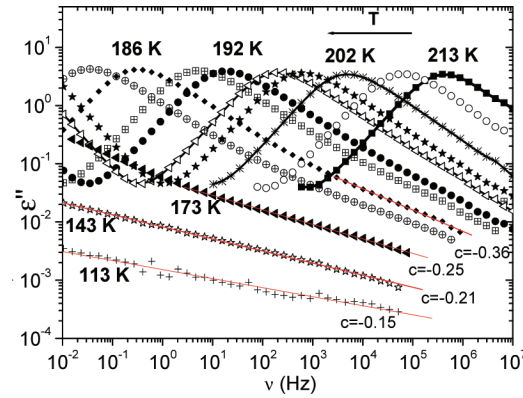

Figure 2. Dielectric loss spectra of quinaldine (QN). Symbols represent experimental data. From right to left: 213, 208, 202, 198, 196, 192, 190, 186, 183, 173, 143, and 113 K. Red lines are from fitting excess wing by power laws, $\varepsilon''(\nu) \sim \nu^{-c}$. The values of c are indicated.

by Hoffmann et al. in glycerol[30] and later is found in more glass formers by others.[31] Here, we show dielectric loss data of N-methyl-ε-caprolactam (NMEC)[32] in Figure 1 and also our own data of quinaldine (QN), a rigid glass former, in Figure 2 and diphenyl-vinylene carbonate (DVPC) in Figure 3. In Figure 1, fits to the α-loss peak at two higher temperature (178 and 180 K) by the one-sided Fourier transform of the Kohlrausch−Williams−Watt (KWW) function,

$$\varphi(t) = \exp[-(t/\tau_\alpha)^{1-n}] \qquad (2)$$

with $n = 0.24$ is shown together with the loss, $\varepsilon''(\nu) \sim \nu^{-c}$, on the higher frequencies. The dashed black line drawn with slope $c = 0.29$ illustrates this feature, which would be called the excess wing or loss with $c \approx 0.2-0.3$ by others.[19,24,27] However, at the lower temperature, the data with comparable losses have a

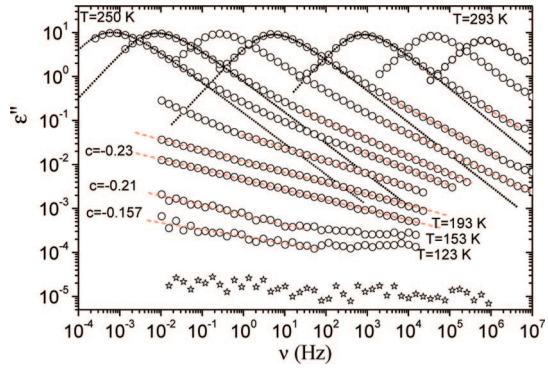

Figure 3. Dielectric loss spectra of diphenylvinylene carbonate (DPVC). Symbols represent experimental data. Open circles from right to left: 293, 283, 273, 263, 258, 253, 250, 243, 213, 193, 153, and 123 K. Dotted lines are the fits by the Fourier transforms of the Kohlrausch functions, $\phi(t) = \exp[-(t/\tau_\alpha)^{1-n}]$, with $n = 0.23$, 0.27, 0.29, and 0.30 (from right to left). Red dashed lines are from fitting excess wing by power laws, $\varepsilon''(\nu) \sim \nu^{-c}$. For the two lowest temperatures, $\varepsilon''(\nu) \sim \nu^{-c}$ has $c \approx 0$ at higher frequencies than about 10^2 Hz to be followed at lower frequencies by $\varepsilon''(\nu) \sim \nu^{-c}$ with $c = 0.21$ and $c = 0.157$. The losses shown, all higher than 10^{-4}, are well within the resolution of the instrument. The empty cell measurement (open stars) showed much lower losses.

steeper slope. This change is made clear in Figure 1 by the other black line drawn with $c = 0.47$ through the loss data taken at the lower temperature of 168 K but still above T_g of NMEC. The significant difference between the slopes of the losses of comparable magnitudes at the two temperatures shows that the shape of the spectrum in this region of the loss is not temperature independent; hence, frequency−temperature superposition of the loss spectra above T_g suggested in ref 24 cannot be achieved. A dashed green line representing ν^{-c} with $c \approx 0.76$ is placed near the lower temperature data at 168 K (green open circles) and is the same as the frequency dependence of the KWW fit to the α-loss peak at 168 K would have. By these constructions in Figure 1, it becomes obvious that the part of the data at 168 K having $\varepsilon''(\nu) \sim \nu^{-c}$ with $c = 0.47$ are in excess of the supposedly KWW fit to the α-loss peak, and it may be called an excess wing. At higher frequencies past this excess wing with $c = 0.47$, there appears a new feature in the spectra having $\varepsilon''(\nu) \sim \nu^{-c}$ with $c \approx 0.1$ and weak temperature dependence of its intensity like the NCL found at higher temperatures and frequencies. There are two possible interpretations of the data.

One interpretation is that the data at 168 K having $\varepsilon''(\nu) \sim \nu^{-c}$ with $c = 0.47$ are not an excess wing but an integral part of the α-relaxation. The observed $\varepsilon''(\nu) \sim \nu^{-c}$ with $c \approx 0.1$ is unrelated to the NCL appearing at GHz frequencies and higher temperatures. Instead, it is the excess wing having the same origin as that found at the higher temperature in Figure 1 with $c = 0.29$. Supposedly, c of the excess wing decreases on decreasing temperature from $c = 0.29$ down to $c \approx 0.1$ in the temperature range shown. Furthermore, the excess wing is interpreted as corresponding to an unresolved β-relaxation.[33] This interpretation was supported by the approximate agreement between the calculated primitive frequency of the CM[33] and the β-relaxation frequency, assuming that the excess wing is part of the unresolved β-relaxation modeled by a symmetric Cole−Cole (CC) empirical function. For NMEC, the primitive frequency has been calculated for each spectrum in Figure 1, and its location is indicated by the vertical arrow in Figure 1. In the previous study of glycerol, propylene carbonate, and propylene glycol,[33] the entire spectrum can be fitted by the additive superposition of the α-loss peak represented by the Fourier transform of a Kohlrausch function and the β-loss peak by a CC function. However, this fitting procedure of adding two independent α- and β-contributions has a problem. This is because the α- and β-relaxations are not independent processes in view of the many correlations existing between the α- and the β-relaxations,[34−36] and especially clear from the results of recent NMR experiments, which show that suppression of part of the JG β-relaxation has the consequence of modifying the α-relaxation.[37,38] Returning to the NMEC spectra at 168 K and temperatures below in Figure 1, the present interpretation says that the higher frequencies part of the data having $\varepsilon''(\nu) \sim \nu^{-c}$ with $c \approx 0.1$ is the excess wing of the unresolved β-relaxation. From the similar frequency dependence of $\varepsilon''(\nu)$ at 168 K and temperatures below shown in Figure 1, we can expect that the dependence, $\varepsilon''(\nu) \sim \nu^{-c}$ with $c \approx 0.1$ or smaller would continue to hold in our experimental frequency range at temperatures much further below 168 K. At such low temperatures, the relaxation frequency of the supposedly unresolved β-relaxation would be many decades below the experimental frequency window. Consequently, the width of the β-loss peak has to be extremely large to account for the anticipated continued observation of the $\varepsilon''(\nu) \sim \nu^{-c}$ with $c \approx 0.1$ or less at lower temperatures. This behavior of the β-relaxation is not easy to justify and seems unlikely.

There is another possible interpretation, alternative to the previous one and actually rationalizing all of the results, including the data of NMEC. Before that, it should be noted that the loss spectra of NMEC are different from the other glass formers having no resolved secondary relaxation including glycerol, propylene carbonate, propylene glycol,[23,33] and quinaldine and diphenyl-vinylene carbonate shown here in Figures 2 and 3. In the same range of loss of NMEC as delineated by the black dashed line at 178 K and the black continuous line at 168 K (see Figure 1), the absolute value of the slope increases on decreasing temperature, corresponding to the change from $c = 0.29$ to $c = 0.47$, respectively. This feature is not found in the other glass formers, where the absolute value of the slope of the excess wing, or c, monotonically decreases with decreasing temperature in any region of the loss[23,30,31,33] (see also Figures 2 and 3). Fits of the α-loss peaks of NMEC for all spectra in Figure 1 by the one-sided Fourier transform KWW function (eq 2) require temperature-independent value of $(1 - n) = 0.76$. Examples of the KWW fits at 178 and 182 K are shown by lines in Figure 1. The green dashed line with a slope of −0.76 placed in the vicinity of the loss data at 168 K (green open circles) is designed to indicate the slope of the high frequency flank of the KWW fit to the α-loss peak at 168 K. By showing this, it is clear that the loss $\varepsilon''(\nu) \sim \nu^{-c}$ with $c = 0.47$ at 168 K may not be considered as part of the α-peak described by the KWW fit as done in the previous interpretation. It is more appropriate to interpret it as the excess loss originating from the unresolved β-relaxation. This is supported by the location of the β-relaxation frequency, $\nu_\beta \equiv 1/(2\pi\tau_\beta)$, calculated from the CM relation, $\tau_\beta = (\tau_\alpha)^{1-n}(t_c)^n$, where $(1 - n) = 0.76$ and $t_c = 2$ ps.[33−35] The location of ν_β(168 K) is indicated by the vertical arrow pointing toward the loss data at 168 K. It can be seen that ν_β(168 K) lies within the loss region defined by the solid black line with the label $c = 0.47$ nearby. This fact supports the interpretation that the loss data at 168 K described by $c = 0.47$ is the excess wing coming from the unresolved β-relaxation but not considered[36b] as part of a CC distribution to be added to the KWW α-loss peak as previously done.[33] The 168 K loss data with slope $c \approx 0.1$ at higher frequencies is then a separate entity, that is, the loss of caged molecules

manifested as the NCL and to be distinguished from secondary relaxation. On increasing temperature, the unresolved β-relaxation increases in dielectric strength but its separation from the α-relaxation becomes lesser due to its weaker temperature dependence of its relaxation time than that of the α-relaxation. The intensity as well as the power law exponent c of the NCL also increase with increasing temperature, as reflected by the increase of the NCL exponent c from 0.1 at 168 K up to 0.29 at 178 K. These increases at higher temperatures are both due to higher anharmonicity of the intermolecular potential and larger amplitudes of fluctuations of the cages. These changes of the β-relaxation and the NCL with increasing temperature are illustrated in Figure 1 by the loss data at 178 K (pale blue squares). The shorter black line that has $c = 0.47$ delineates the region of data that has slope of -0.47, and the vertical arrow indicating ν_β(178 K) of the unresolved β-relaxation again lies within the region. By these constructions in Figure 1, we show the excess wing at 168 K with $c = 0.47$ is still present at 178 K, albeit its frequency domain is curtailed on the low frequency side by the encroaching KWW α-loss peak and on the high frequency side by the rising NCL. The power law with $c = 0.29$ at 178 K is due to the NCL contribution that becomes $c = 0.1$ at 168 K and below. Our interpretation of dielectric spectra of glass formers not having its β-relaxation resolved is that the loss of caged molecules exemplified as the NCL is omnipresent.[21] The NCL transpires at times before the unresolved β-relaxation, which terminates it by causing the cages to decay.[21] This interpretation applies as well to glycerol,[30,33] propylene carbonate,[31,33] quinaldine, and diphenyl-vinylene carbonate (DPVC) shown here in Figures 2 and 3, despite some difference in the isothermal loss spectra of these glass formers from that of NMEC. In particular for DPVC, loss spectra at 153 and 123 K in Figure 3 show unequivocal evidence for a distinct NCL with $c \approx 0$ at frequencies higher than 10^2 Hz to be followed at lower frequencies below 10^2 Hz by the excess wings, $\varepsilon''(\nu) \sim \nu^{-c}$, with $c = 0.21$ and $c = 0.157$, respectively. The loss data of DPVC showing the NCL, although only slightly higher than 10^{-4}, are well within the experimental sensitivity of the instrument used in the dielectric measurements. This is another evidence that there is still an excess loss with a larger c associated with the unresolved β-relaxation at lower frequencies after termination of the NCL. In this interpretation, the dielectric NCL observed in all of these glass formers [i.e., $\varepsilon''(\nu) \sim \nu^{-c}$ with $c \approx 0.1$ or less observed at frequencies below 10^6 Hz and at lower temperatures down to the glassy state] has the same origin as NCL observed at higher temperatures and frequencies by dynamic light scattering and OHD-OKE.

NCL in some other glass formers has low dielectric loss at low temperatures, but it still can be detected by a highly sensitive spectrometer (like the AH 2700A bridge from Andeen-Hagerling) albeit in the limited frequency range of 10^1-10^4 Hz. Using this spectrometer, the NCL was detected in PI[39] at temperatures below T_g where the α- and β-relaxations have been moved far outside the frequency window. This is truly a NCL located at higher frequencies than the resolved β-relaxation, and it is certainly not an excess wing. Found dielectrically in the low frequency range of 10^1-10^4 Hz, this NCL should be the same as the NCL of PI observed before by dynamic light scattering[20] in the GHz range at temperatures above and below T_g mentioned above. Had an instrument been available to detect the NCL of PI in the intermediate frequency range from 10^4 Hz to 1 GHz, we expect it would be found at temperatures below T_g. The anticipated data would interpolate the dielectric data in 10^1-10^4 Hz range and the dynamic light scattering data in the GHz range.

Picosecond acoustic transmission measurements of high frequency structural relaxation in supercooled glycerol,[40] in the frequency range of 2−20 GHz and temperatures between 235 and 291 K, also demonstrated the presence of additional relaxation not accounted by either the α-relaxation or the β-relaxation of the idealized mode-coupling theory. The analysis of the data demonstrated that this additional relaxation is the NCL in the susceptibility spectrum of supercooled glycerol, supporting the findings of the dynamic light scattering measurements.[22]

In 2003,[15] additional observations of IPL, pt^{-1+c} with $c \ll 1$, by OHD-OKE in the supercooled liquids, BZP, and 2-biphenylmethanol (BPM) were presented, together with refurbished IPL data that were previously obtained on *ortho*-terphenyl (OTP),[41] salol,[14] and dibutylphthalate (DBP).[42] Depolarized light scattering (DLS) experiments on BZP reported good agreement with the OHD-OKE results.[24] The observed IPL may be consistent with the logarithmic decay of orientation correlation function obtained by a special solution of MCT near a high order singularity.[9] However, this way to explain the IPL was abandoned[15] because this solution by MCT may apply only in very rare situations for systems that have special interparticle interaction potentials such as colloids, while the logarithmic decay was found in the five glass formers with different chemical structures and interaction potentials. The amplitude p of IPL in all of the five glass formers increases weakly with temperature. This may not be obvious from the way that the T-dependence of p was forced to be fitted to $(T - T_c)^{1/2}$ suggested by MCT in ref 15. It turns out that a linear dependence on T is also an acceptable description of the data. For example, p of salol only increases by a factor of about 3 when T increases from 260 to about 330 K, similar to the weak T-dependence of the NCL found in PIB, glycerol, and PMMA by dynamic light scattering.[18,20−22] Thus, the OHD-OKE data of glass formers with different chemical structures support the universal presence of NCL or IPL with $c \ll 1$ having general properties.

In 2004, by including rotation-translational coupling in a schematic model, Götze and Sperl[10] and later on Sperl[11] showed that the IPL data of salol and BZP from OHD-OKE could be explained by the nearly logarithmic decay of correlation function obtained from the two-correlators model of MCT. One correlator is for density fluctuations and the other for reorientational fluctuations of the molecules. By assuming the presence of strong rotational−translational (RT) coupling, the model yields time dependence of response functions in agreement with those measured for BZP and salol by OHD-OKE. They demonstrated that the fast β-relaxation of MCT can lead to a symmetrical CC loss peak[43] with its high frequency flank having the frequency dependence of ν^{-c}. The conventional susceptibility loss minimum scenario of the idealized MCT results if the CC loss peak frequency is larger than the microscopic excitations, and the data can be fitted by the idealized MCT as usual. According to the new two-correlators model of MCT,[10,11] the CC loss peak with frequency dependence given by the imaginary part of $1/[1 + (i2\pi\nu\tau_{CC})^c]$ also can be located at much lower frequencies. In this case, the high-frequency flank of the CC peak gives rise to a weaker power law ν^{-c} (i.e., either an excess wing or logarithmic decay if $c \approx 0$) on the high-frequency side of the α-loss peak[44,45] (see Figure 1 in ref 45). It was shown[11] that this scenario can fit the IPL data of BZP from OHD-OKE. DLS experiments on BZP reported good agreement with OHD-OKE in showing the power law ν^{-c} indicating the excess wing.[19]

The recent 2007 broadband dielectric measurements of BZP[44,45] indeed found a symmetric CC peak at low temperatures

(200 K and below). At higher temperature, it tends to merge with the α-loss peak and was seen as an excess wing from 210 to 225 K. However, the characteristics of the dielectric CC relaxation depart from that of the MCT CC relaxation. These include the following two points.[44,45] (i) The relaxation time of the MCT CC peak from the MCT analysis of the OKE data at 251 K is about 2 orders of magnitude shorter than that of the dielectric CC peak obtained by extrapolation to the same temperature. (ii) The frequency and width of the MCT CC peak should be temperature independent, while that of the dielectric CC peak in BZP are strongly temperature dependent, and the width parameter c reaches values outside the range allowed by MCT. Other problems of the two-correlators MCT explanation of the excess wing were pointed out in refs 19, 24, and 27. Although the IPL or the excess wing can be successfully reproduced by the theory at temperatures above the MCT critical temperature T_c, the excess wing continues to be observed in BZP and other glass formers at lower temperatures down to T_g. According to refs 19, 24, and 27, this poses another problem for this recent version of MCT because still it cannot explain the characteristics of dynamic susceptibility at longer time scales and lower temperatures down to T_g.

Let us compare the BZP dielectric data of Lunkenheimer et al.[44] and Pardo et al.[45] at 250 K with the OHD-OKE spectra at 251 K. The highest frequency in the dielectric measurements at 250 K is about 2 GHz (corresponding to ∼100 ps). The IPL, pt^{-1+c} with $c = 0.13$, found by OHD-OKE at 251 K, occurs in the time regime shorter than about 10 ps. Thus, dielectric relaxation measurements were not able to see the IPL in the form of the NCL, which would be $\varepsilon''(\nu) = p'\nu^{-c}$ with $c = 0.13$, the equivalent of IPL, pt^{-1+c} with $c = 0.13$, found by OHD-OKE. Dielectric measurement is not able to see the excess wing that follows after the NCL in time either. This is because the former occurs in the intermediate time regime longer than 10 ps and shorter than 10^2 ps (see Figure 3 in ref 44). Despite the inability of Lunkenheimer et al. and Pardo et al. to measure the complex dielectric permittivity $\varepsilon^*(\nu)$ at frequencies higher than 2 GHz at low temperatures in their experiment on BZP, a special experimental method using a circular parallel-plate capacitor was able to measure the $\varepsilon^*(\nu)$ at the frequencies from 100 MHz to 20 GHz for five glassy polymers, PMMA, polystyrene (PS), polyethylene terephthalate (PET), polyethylene naphthalate (PEN), and polyvinylchloride (PVC), at room temperature by Nozaki and co-workers.[46a] Power law dependence of the loss factor with very small exponent c was found in these polymers in the glassy state, which is definitely identifiable with the NCL. Combining this high-frequency dielectric technique with conventional lower frequency measurements, Nozaki and co-workers[46b] were able to find the NCL with $c \approx 0.1$ of sorbitol and xylitol in the glassy states that essentially pervades the entire frequency range from 2 GHz down to 100 Hz. For sorbitol, such a vast expanse of the NCL was found at 183, 163, and 143 K. The β-relaxation time of sorbitol has been determined in the glassy state,[46c] and it has the Arrhenius temperature dependence given by $\tau_\beta/s = 1.3 \times 10^{-17}\exp(E_\beta/RT)$ with $E_\beta =$ 61 kJ/mol. At 143 K, $\log_{10}(\tau_\beta/s)$ calculated by the Arrhenius relation is equal to 5.4, and the frequency of the β-loss maximum ν_β would be located at about 10^{-6} Hz. If the β-relaxation represented by a symmetric CC function were assumed to be responsible for the observed NCL, its half-width-at-half-maximum is at least 15 decades. This immense width is not easy to comprehend or justify. Published isochronal dielectric loss data of xylitol at 10 kHz also by Nozaki and co-workers[46d] (see Figure 3a in this reference) capture the α-relaxation peak and the β-relaxation (previously resolved in isothermal dielectric loss measurements,[46c] and $\log(\epsilon'')$ exhibits the $\exp(T/T_0)$ dependence at lower temperatures down to the lowest temperature of measurement of about 70 K. The β-relaxation time of xylitol has been determined in the glassy state,[46c] and it has the Arrhenius temperature dependence given by $\tau_\beta/s = 10^{-15}\exp(E_\beta/RT)$ with $E_\beta = 52$ kJ/mol. At 150, 100, and 70 K, $\log_{10}(\tau_\beta/s)$ calculated by the Arrhenius relation is equal to 3.1, 12.2, and 23.8, respectively. If the β-relaxation were responsible for the observed loss at 10 kHz [equivalent to $\log_{10}(\text{time}/s) = -4.8$] and assuming it is represented by a symmetric CC function, its loss maximum would be 7.9, 17, and 28.6 decades of frequency below 10 kHz at temperatures 150, 100, and 70 K, respectively. The corresponding complete span of the symmetric CC function would be twice as large. Thus, unthinkably huge breadths of the β-relaxation are needed to account for the observed loss data of xylitol at these lower temperatures. This is highly improbable and hence also is the hypothesis that the high-frequency (excess) wing attributed to the β-relaxation is responsible for the observed loss having the $\exp(T/T_0)$ temperature dependence at temperatures below 150 K. Instead, the results are additional proof that the NCL is a separate and fundamental process of glass-forming substances that should be distinguished from the loss in excess of the KWW α-relaxation coming from processes involving cooperative motion of increasing number of molecules and initiated by the JG β-relaxation.[21,35,36b]

DLS data at frequencies higher than 200 MHz and temperatures in the same range of OHD-OKE data were obtained by Brodin et al.[19,24,27] for salol and BZP, and the results are in agreement with that from OHD-OKE studies. However, the view on the IPL by these authors is different from us and others. They consider the exponent c of the IPL, pt^{-1+c}, to be temperature-independent with $c \approx 0.2$, seen by dielectric relaxation as the excess wing, $\varepsilon''(\nu) \sim \nu^{-c}$, at lower temperatures. This view ignores the observations of the exponent c are nearly zero in many cases, including salol by OHD-OKE at 247 K,[14,15] PIB,[18] PI,[20] glycerol, and PMMA[22,47] by DLS over a range of temperatures above and below T_g, glycerol by picosecond acoustic transmission measurements[40] in the frequency range 2−20 GHz and $235 < T < 291$ K, and five amorphous polymers from 100 MHz to 20 GHz at room temperatures by a special microwave technique.[46] There is no doubt that the excess wing with c having nonzero values and even ≈0.2 shows up often in dielectric loss spectra of glass formers in some temperature and frequency ranges, but it may originate from different mechanisms. For one, the excess wings of BZP in dielectric loss spectra by Pardo et al. at temperatures from 210 to 220 K are actually the high-frequency wing of a broad secondary relaxation, the presence of which is certain because it has been resolved at lower temperatures and in the glassy state. However, this secondary relaxation is not the JG β-relaxation of BZP, as we shall show in a later section. Even if the high-frequency flanks of the resolved secondary relaxation in BZP are forced to be interpreted as excess wings corresponding to IPLs, pt^{-1+c}, the exponent c changes with temperature (see Figure 2 of ref 45). For glass formers that have no resolved secondary relaxation such as glycerol, propylene carbonate (PC), picoline, and propylene glycol discussed by Brodin et al., as well as NMEC, QN, and DVPC shown in Figures 1−3, the excess wing with $c \approx 0.2$ was found at some temperatures near and above T_g, but c changes with temperature (see Figures 1−3). From the above discussion, it is clear that IPL seen by OHD-OKE and DLS or the excess wing in dielectric spectra with c

≈ 0.2 can originate from different causes and is a transitory feature because c is not a constant. Therefore, it cannot be considered as fundamental.

Invariably, there is the NCL with $c \approx 0$ showing up at higher frequency than the excess wing, whichever is the cause. This is especially evident in the spectra at temperatures below T_g (for glycerol, see ref 30; for PC, see ref 31; and for picoline, see ref 48). All of these examples indicate that the NCL is a faster process occurring before the excess wing and for sure can be seen in dielectric spectroscopy when the excess wing is moved out of the experimental frequency window at lower temperatures. The excess wing corresponds to the dynamics in transition when passing in time from the NCL where all molecules are caged to the (unresolved) JG β-relaxation where molecules are no longer caged. Thus, the excess wing reflects the contribution to the loss from the decay of cages caused by the onset of the unresolved JG β-relaxation. The time when the cages start to decay marks the termination of the NCL regime.[49,50] The JG β-relaxation belongs to a special class of secondary relaxations satisfying certain criteria established in ref 51 such as the motion involving the entire molecule and properties mimicking that of the α-relaxation, which will be elaborated in the next section. There, we show that the JG relaxation frequency is located either near or on the excess wing, and it marks the time of total dissolution of cages through local relaxation by rotation and/or translation of essentially the entire molecular unit. In other words, the excess wing represents the transitory relaxation processes causing the decay of the cages and ushering in the true relaxation regime first seen as the JG β-relaxation, which is followed by motions involving increasing number of molecules terminating in the cooperative KWW α-relaxation with maximum length scale allowed by the intermolecular potential.

In the case of OHD-OKE experiments carried out at higher temperatures, the JG β- and α-relaxations have already merged together, and it is the merged relaxation that terminates the IPL having exponent c, which decreases toward the value $c \approx 0$ with decreasing temperature. The merged relaxation is given by the term $t^{-1+b}\exp(t/\tau_\alpha)$ in eq 1, which in the frequency domain corresponds to imaginary part of the Cole−Davidson function, $1/(1 - i\omega\tau_\alpha)^b$. Such action of the merged JG β- and α-relaxation in terminating the IPL can be seen by the other product term, $pt^{-1+c}\exp(-t/\tau_\alpha)$, needed in the function given by eq 1 to fit OHD-OKE data. The factor $\exp(-t/\tau_\alpha)$ in the product effectively ends the contribution of the IPL pt^{-1+c} at time longer than τ_α. The action ensures that the term, pt^{-1+c}, is not an additive contribution to the merged β- and α-relaxation, a fact that has been shown before in the context of NCL (i.e., when $c \approx 0$) from a combined consideration of DLS and dielectric relaxation data of the glass-forming molten salt, $Ca_{0.4}K_{0.6}(NO_3)_{1.4}$.[52]

It is interesting to put together the observation of NCL in $\chi''(\nu)$ of glycerol ($T_g = 185$ K) at 160 K by DLS in the 1−40 GHz range by Kisliuk et al.[22] (see Figure 1b in this reference) and also in $\varepsilon''(\nu) = p\nu^{-c}$ with $c \approx 0.07 \pm 0.02$ at nearly the same temperatures by dielectric spectroscopy in the 10^{-2} to 10^5 Hz range by Kudlik et al.[31] (see Figure 3 and eq 7 in this reference). The NCLs observed in these two widely different frequency ranges at the same temperature have the same property and are likely exemplification of the same physical process. Although no data of either $\chi''(\nu)$ or $\varepsilon''(\nu)$ were obtained in the intermediate frequency range from 10^5 to 10^9 Hz, if measurable at 160 K, in all likelihood, they are also NCL interpolating the low frequency $\varepsilon''(\nu)$ data and the high frequency $\chi''(\nu)$ data. This is because there is no other relaxation process in glycerol that will appear within the intermediate frequency region at 160 K that one can think of. The excess wing and the α-loss peak of glycerol at 160 K are located at much lower frequencies way below 10^{-2} Hz. The result indicates that NCL pervades over the entire frequency range from 10^{-2} Hz to 40 GHz at 160 K and lower temperatures.

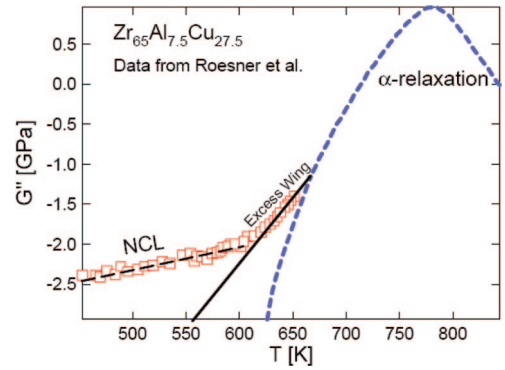

Figure 4. Isochronal mechanical loss modulus $G''(T)$ of $Zr_{65}Al_{7.5}Cu_{27.5}$ showing three distinct contributions: the dominant α-loss peak, the excess wing, and the NCL (open squares). Data are taken from Rösner et al. (ref 53).

Thus, from the discussion given above, NCL is a universal and fundamental feature in the dynamics of glass-forming substances although it is harder to detect than other processes including the excess wing because of its lower intensity and/or location at higher frequencies. Nevertheless, NCL should be distinguished from the excess wings with c not close to zero, particularly those having temperature-independent exponent $c \approx 0.2$ proposed to be universal by Brodin et al. It is true that the excess wing is a general feature of glass formers having no resolved secondary relaxation as stressed by Brodin et al. However, it is just a feature of the dynamics transpiring after the NCL. Not often, these two features can be seen together in the isothermal spectrum because of limitation in the width of the frequency window and low intensity of the NCL. The isochronal spectrum of the loss as a function of temperature at a fixed frequency can better show the simultaneous presence of the NCL and the excess wing. An interesting example is the isochronal mechanical loss G'' spectrum of the metallic glass $Zr_{65}Al_{7.5}Cu_{27.5}$ presented in Figure 4, which shows the presence of both the excess wing and the NCL.[53−55] The latter is identified in the semilog plot of G'' vs T by its characteristic weak T dependence, approximately proportional to $\exp(T/T_0)$, also found in several molecular glass formers by dielectric, mechanical, and spin−lattice relaxation spectroscopies (see Figure 6 in ref 31). Our interpretation of the isochronal $G''(T)$ spectrum of $Zr_{65}Al_{7.5}Cu_{27.5}$ showing the presence of both the excess wing and the NCL was in accord with that given by Hachenberg and Samwer for the "fragile" metallic glass $Pd_{77}Cu_6Si_{17}$ (see Figure 1 in ref 54). It should be mentioned that although we, as well as Hachenberg et al., interpret the part of the $G''(T)$ of metallic glasses that has the $\exp(T/T_0)$ dependence as the NCL, an alternative interpretation was given in the earlier publication by Rösner et al.[53] These authors considered the same part of the $G''(T)$ spectrum of $Zr_{65}Al_{7.5}Cu_{27.5}$ not as the NCL but the continuation of the excess wing associated with the β-relaxation to lower temperatures in the glassy state. The observed $\exp(T/T_0)$ dependence was interpreted as due to change in temperature dependence of the excess wing intensity after entering into the glassy state by analogy to change of the temperature dependence of the amplitude of the faster processes, including relaxation

strength of secondary relaxation,[25] NCL intensity,[21] and mean square displacement[21] measured by neutron scattering. Therefore, the observed $\exp(T/T_0)$ dependence in metallic glasses could be due to change of T dependence of the amplitude of excess wing after crossing T_g. We have discussed before the isochronal dielectric loss $\epsilon''(T)$ data of xylitol at 10 kHz from ref 46d. The spectrum (see Figure 3a in ref 46d) resembles in every respect the isochronal mechanical loss modulus $G''(T)$ of the metallic glass $Zr_{65}Al_{7.5}Cu_{27.5}$, shown here in Figure 4. From the analysis of the isochronal $\epsilon''(T)$ data of xylitol at low temperatures, we have shown that the observed $\exp(T/T_0)$ dependence is highly unlikely to come from the excess wing associated with the β-relaxation. It is tempting to draw the same conclusion on the metallic glasses, but this cannot be made at the present time because the $G''(T)$ data had not been obtained at sufficiently low temperatures like in the case of xylitol. Only when data of $G''(T)$ at much lower temperatures become available in the future and if $G''(T)$ continues to have the $\exp(T/T_0)$ dependence, then the same conclusion can be made. In any case, the possible presence of both the excess wing (or IPL with $c \approx 0.2$ or other values) and the NCL (IPL with $c \approx 0$, or logarithmic decay of orientation correlation function) in metallic glass is interesting because there is no rotation. Hence, RT coupling is absent in metallic glasses, and the recent versions of MCT[10,11,56] that incorporate RT coupling cannot explain the IPL with $c \approx 0.2$ or NCL with $c \approx 0$ in Figure 4.

The following is a legitimate question to be asked: Why did OHD-OKE produce data that deviate from the traditional and idealized MCT while other techniques like quasielastic neutron scattering,[57−60] and dynamic light scattering[7,8,61−63] earlier have found the idealized MCT works in the same fragile glass former such as salol and OTP? The experiments that reported agreement with the idealized or extended MCT predictions include DLS on salol,[7,62] OTP,[63] and $Ca_{0.4}K_{0.6}(NO_3)_{1.4}$ (CKN)[7,64] and neutron scattering on OTP[59,60] and CKN.[64] The answer is that the much wider spectral range of OHD-OKE (from subpicoseconds to about 5×10^5 ps in the case of salol) allows meaningful spectra at lower temperatures to be collected. At the lowest temperature such as 247 K for salol in OHD-OKE experiment, the α-relaxation time τ_α is even longer than the upper bound of the time window. This favorable situation at 247 K makes possible for the true caged dynamics, exemplified as IPL with $c \approx 0$ (logarithmic decay or NCL), to be observed over a broad frequency range and clearly identified. The OHD-OKE data for τ_α of OTP at 284 K are again very long and about 10^5 ps, and the corresponding IPL has $c = 0.15 \pm 0.03$. On the other hand, the experimental windows of neutron scattering (<200 ps)[59,60] and DLS ($\nu > 0.1$ GHz)[7,62,63] are limited to much shorter times or higher frequencies, and data were usually performed at higher temperature whereby the merged JG β- and α-relaxations or its high-frequency flank appears in the susceptibility spectrum $\chi''(\nu) \propto \mathrm{Im}\{1/(1 - i\omega\tau_\alpha)^b\}$ and is seen as the von Schweidler law with $\chi''(\nu) \propto \nu^{-b}$, where b is the same as that appearing in eq 1. Encroachment of the high-frequency flank of the α-relaxation from the low-frequency side into the already limited experimental frequency window leaves no room for the NCL to be observed in the neutron and dynamic light scattering experiments in the past. The consequence is necessarily the observation of a susceptibility minimum and its characteristics, including the exponents b and a of the power laws defining it, which had been compared favorably with the predictions of the idealized MCT in the years before the advent of the OHD-OKE data.

Broadband dielectric relaxation measurements of CKN[65−67] have the advantage of immense frequency range from as high as 4×10^{11} Hz to as low as typically 10^{-2} Hz. For frequencies higher than 0.1 GHz and temperatures above the putative MCT critical temperature $T_c = 375$ K, the dielectric loss spectra exhibit minima consistent with neutron scattering and DLS[7,62] in the same spectral range. However, at lower temperatures, the NCL appears in the dielectric loss spectra over an increasing range of frequencies with decreasing temperature.[21,49,69,70] At 361 K, $\varepsilon''(\nu)$ already exhibits a very flat minimum from 10^{10} to 10^8 Hz. The NCL is even more evident in $\varepsilon''(\nu)$ at lower temperatures. At 342.5 K, the NCL extends from 10^9 Hz down to 10^6 Hz. The latter corresponds to about 10^5 ps, which is also the longest time in OHD-OKE experiments. Thus, like salol and OTP, one scenario of MCT (i.e., the CC peak frequency is higher than that of the microscopic peak) is needed to explain the neutron scattering and DLS data of CKN, and the other scenario (i.e., CC peak located at much lower frequencies) to account for the dielectric relaxation data of CKN.

Caging is not unique to interacting molecules in glass formers but also occurs in other interacting systems such as colloidal particles in suspension and ions in ionically conducting glasses and crystals.[69,70] The NCL or IPL with $c \ll 1$ were found in these other systems through the time dependence of the mean square displacement $<r^2(t)>$. For a colloidal glass at packing fraction of 0.62, the confocal microscopy data[71] of $<r^2(t)>$ presented in a log−log plot clearly shows the t^c dependence with c decreasing with increasing aging time to reach values of 0.13 (see Figure 1 of ref 72), which is followed at longer times by a more rapid increase with $c = 0.35$ corresponding to what may be called the analogue of the excess wing of molecular glass formers. Plenty of dielectric relaxation measurements of dielectric loss $\varepsilon''(\nu)$ in ionically conducting glasses and crystals have found the NCL of caged ions at sufficiently high frequencies or low temperatures.[49,69,70,73] MD simulations show $<r^2(t)>$ has the t^c dependence with c decreasing with decreasing temperature[70] analogous to the behavior found for the IPL by OHD-OKE.

The results presented in this section indicate that the NCL in the susceptibility loss spectrum or IPL with $c \ll 1$ in the OHD-OKE response function is a universal feature of the dynamics in the caged regime. It is the loss due to motions of molecules confined within the anharmonic potential of the cages and the fluctuations of the cages themselves with time. Unlike rotational and translational motions involved in secondary and primary relaxations, this loss inside cages has no characteristic time and hence continues indefinitely until the cages start to decay by the onset of a secondary relaxation involving the motion of the entire molecule, which is the JG β-relaxation.[49−51] This is evidenced by the fact that the JG β-relaxation frequency estimated by the primitive relaxation frequency of the CM is located below but not far from the lower bound of the frequency regime of the NCL[35,49] (see also Figure 1 herein). The interconnection between the NCL and the JG β-relaxation is thus clear. In the transition region from NCL to either the unresolved or the resolved JG β-relaxation, the loss may appear as an excess wing. Anharmonicity of the intermolecular potential as well as fluctuations of cages generally decreases with decreasing temperature; hence, the magnitude of the NCL decreases with decreasing temperature. In addition, the JG β-relaxation that terminates the caged regime is moving to longer times or lower frequencies with decreasing temperature, and thereby, the NCL can be seen over more decades of time/frequency. These two factors are responsible for the observed decrease of exponent c with decreasing temperature and the weak temperature dependence of the intensity of the NCL seen

in the OHD-OKE experiments and also in dielectric relaxation measurements (see Figures 1−3). In support of this interpretation, we cite the experimental evidence of cage fluctuations or rearrangements and cage decay in colloidal particles suspension obtained from direct observation of motions by confocal microscopy experiment.[74] A model of a caged particle that has its cage decaying very slowly with time was solved numerically, and a NCL over many decades of frequency was reproduced.[75] Admittedly, this model is artificial, and it can only serve the purpose of stimulating the construction of fundamental model of caged dynamics in the same spirit.

4. Secondary Relaxation that is Correlated with the Primary α-Relaxation

Traditionally, secondary relaxation is considered to be processes uncorrelated with the primary α-relaxation and hence unimportant for glass transition. However, more detailed studies of secondary relaxations in glass formers of all kinds have revealed that a certain class of them may be important.[51] The secondary relaxations in this class distinguish themselves by either having properties mimicking those of the primary α-relaxation or bearing nontrivial correlations with the α-relaxation. For a summary of these properties found prior to 2004, see the review given in ref 51. To honor the pioneering work on secondary relaxations done by Johari and Goldstein,[76,77] especially their discovery of secondary relaxation in totally rigid molecules, it was proposed to call this special class the JG β-relaxations.[51] This nomenclature is to be distinguished from other workers who use the same term for *any* secondary relaxation to differentiate it from the fast β-relaxation of idealized MCT. If more than one secondary relaxation are present, usually the slowest one is the JG β-relaxation because it likely involves the motion of essentially the entire molecule. The faster one, naturally called the γ-relaxation, involves the motion of only a part of the entire molecule, and its properties are uncorrelated with that of the α-relaxation.[50,51] Here, we mention as examples two properties of the JG β-relaxation that distinguish it from the non-JG secondary relaxation and were known before 2004. They are (i) significant increase of its relaxation time, τ_{JG}, on elevating pressure and (ii) the approximate agreement[49,51,78−81] of τ_{JG} with the primitive relaxation time τ_0 calculated from the CM relation,[82−84]

$$\tau_\alpha = [t_c^{-n}\tau_0]^{1/(1-n)} \quad (3)$$

that is, $\tau_{JG} \approx \tau_0$. In eq 3, τ_α is the α-relaxation time and $(1-n)$ is the fractional exponent of the KWW function (eq 2), used to fit the correlation function of the α-relaxation, and $t_c \approx 2$ ps for molecular and polymeric glass formers. Since the publication of the review of JG β-relaxation in 2004,[51] the discovery of other properties has strengthened the belief of the fundamental importance of the JG β-relaxation. For example, by dielectric relaxation measurements on varying both temperature T and pressure P while keeping τ_α constant, it was found that the shape of the α-loss peak (or equivalently, n in the Kohlrasuch function that fits it)[35] as well as τ_{JG}[85,86] are both invariant to different combinations of T and P. These remarkable properties are consistent with the CM (eq 3)[35,85] when combined with the relation $\tau_{JG} \approx \tau_0$. Because it was possible to elevate P by 4 orders of magnitude together with large compensating increase in T to maintain τ_α constant in these experiments, the density and entropy vary over a large range; yet, the dispersion of the α-relaxation and the ratio τ_α/τ_{JG} is unchanged. These experimental findings point to the fundamental importance of the frequency dispersion or time dependence of the α-relaxation (or its surrogate n in the KWW function) and also the JG β-relaxation from its strong correlation with the α-relaxation. Using a deuteron magnetic resonance technique of spin−lattice relaxation weighted stimulated-echo spectroscopy, Böhmer and co-workers[37,38] were able to show that the α-relaxation can be modified by suppressing the contributions of some subensembles of the JG β-relaxation in sorbitol, OTP, and cresolphthalein dimethylether (CDE). This NMR result is more clear evidence for a correlation between the JG β-relaxation and the α-relaxation among others.[34,49,51,87]

The experimental evidence of the importance of the JG β-relaxation also was recognized by others as appeared in further work[56] on the schematic MCT, which incorporates RT coupling to explain the nearly logarithmic decay observed in OHD-OKE data.[10,11] The work[56] showed that this version of MCT also predicts the presence of the excess wing with its slope decreasing with decreasing temperature and gradually evolves into a JG β-peak with increasing RT coupling. However, the excess wing was found in metallic glasses[53−55,88,89] (see also Figure 4) and JG β-relaxation in plastic crystals.[81,90] However, there is no RT coupling in these glass formers. Also, it is not clear whether the MCT with RT coupling can explain the established relations between the JG β-relaxation and the α-relaxation.[49−51,78,79,85,86] A secondary relaxation was produced by another schematic mode coupling theory in which the ideal glass transition is cut off by a decay of the quadratic coupling constant in the memory function.[91] The secondary relaxation produced remains at a constant frequency, while the α-relaxation moves to lower frequencies. This behavior of the secondary relaxation indicates that it is not correlated with the α-relaxation and is not the important JG β-relaxation that we know of.

The glass formers studied by OHD-OKE have attracted attention because of the discovery of the IPL with $c \ll 1$ (or nearly logarithmic decay) and the explanation by MCT with RT coupling. These include BZP,[15] DBP, and salol. We now go further by considering various other properties observed in these three glass formers that have impacts on fundamental understanding and theoretical interpretation. Properties observed or not observed in these three glass formers, as well as the issues raised on understanding them are discussed in this section in connection with the question on the universality and fundamental importance of the JG β-relaxation. Properties of the α-relaxation will be discussed in the next section.

Pardo et al. and Lunkenheimer et al.[44,45] have made the state-of-the-art broadband dielectric measurement of BZP ($T_g \approx 212$ K). They found a very broad secondary relaxation that is well-resolved at 210 K and temperatures below down to 180 K in the glassy state. Is this the JG β-relaxation? To answer this question, the authors of ref 44 make use of one of the criteria[51] of approximate agreement of the observed relaxation time τ_{obs} with the τ_0 calculated by eq 3 from τ_α and the stretch exponent $(1-n)$ in the KWW function, the Fourier transform of which fits the α-loss peak. These KWW parameters used were deduced from the corresponding parameters of the Cole−Davidson function[44] actually used to fit the data at temperatures ≥215 K, the calculated τ_0 is slightly longer than τ_{obs} at higher temperatures and is an order of magnitude longer than τ_{obs} at 215 K. From the apparent approximate agreement, it was concluded that the observed secondary relaxation is the supposedly universal JG β-relaxation of BZP. However, comparison of τ_0 with τ_{obs} was not made at temperatures lower than 215 K where τ_{obs} had been determined with precision because the maximum of the secondary loss peak shows up in the spectrum. Direct fit of the loss peak at 215 K by the one-sided Fourier transform of

the KWW function, emphasizing good fit on both sides of the main peak and particularly the low frequency flank, requires the stretch exponent $(1-n)$ to have the value of 0.70. Assuming the value of $(1-n)$ is also 0.70 at temperatures near T_g (i.e., the frequency dispersion of the α-relaxation does not change) our calculated τ_0 at 210 K is about 10^{-3} s, which is about two and half-orders of magnitude longer than τ_{obs}. At lower temperatures, the deviations are even larger. For example, from τ_α of about 10^5 s at 200 K given in Figure 2 of ref 44, the calculated τ_0 is approximately 10^{-1}s, which is about 4 orders of magnitude longer than τ_{obs}. It is true that well below T_g, the system can fall far from equilibrium, but eq 3 as well as the relation $\tau_{JG} \approx \tau_0$ continues to hold. There are cases where the structural relaxation time τ_α was obtained at temperatures below T_g, and the calculated τ_0 values are in good agreement the observed τ_{JG}.[106,107] Thus, from our evaluation, the observed secondary relaxation is not the JG β-relaxation of BZP but the faster γ-relaxation. If the former exists, its relaxation time τ_{JG} is closer to τ_α than τ_{obs}. In the dielectric loss spectrum, this means that the JG β-relaxation frequency, $\nu_{JG} \equiv 1/(2\pi\tau_{JG})$, is located on the high frequency flank of the α-loss peak, sandwiched between the α- and the γ-relaxations; hence, the JG β-relaxation cannot be resolved. This situation of not having a resolved JG β-relaxation in BZP is like that found in NMEC, QN, and DPVC (shown before in Figures 1−3), glycerol, propylene carbonate, and propylene glycol,[92] except in these other glass formers there is no γ-relaxation. Nevertheless, the common feature is that they all have narrow α-loss peaks or small n.

Our rationalization given above for not being able to resolve the JG β-relaxation of BZP is by using the CM prediction that $\tau_{JG} \approx \tau_0$, and the fact that the calculated value of τ_0 by eq 3 is too close to τ_α because the coupling parameter $n \approx 0.3$ is too small. In fact, $\nu_{JG} \approx \nu_0 \equiv 1/(2\pi\tau_0)$ obtained from the calculated τ_0 falls on the high-frequency flank of the α-loss peak at location where the data are in excess of the KWW fit. Although this is a possible rationalization of the problem of not observing the supposedly universal JG β-relaxation in the dielectric spectrum of BZP, it is far from being totally satisfactory. One way to give a better chance of resolving the JG β-relaxation of BZP is to enhance the coupling parameter n of BZP. Then, according to eq 3, the ratio $(\tau_\alpha/\tau_0) \approx (\tau_\alpha/\tau_{JG})$ becomes larger and the JG β-relaxation and the α-relaxation are separated further apart. One proven method to enhance the coupling parameter of a glass former is to mix BZP as minority guest molecules with another glass former serving as the majority host and having lower mobility or higher T_g. The slower host molecules retard the motion of the guest molecules further more, and thereby stretch the α-relaxation correlation function of the BZP guest molecules to longer times. The consequence of the stretching is that the α-relaxation correlation function of the BZP guest in the mixtures has a smaller exponent $\beta_{KWW} \equiv (1-n)$ when fitted by the Kohlrausch function (eq 2) or larger n (assuming concentration fluctuations are unimportant in mixtures with dilute amount of BZP). If the host is apolar like oligomers of styrene and the guest like BZP is highly polar, dielectric spectroscopy is the choice because it monitors exclusively the dynamics of the polar guest molecules. The theoretical basis of this method was laid out in ref 93, and the effect has been demonstrated for polar guest molecules including picoline,[93,94] TBP, and QN.[95] Also, a MD simulation[96] has verified this prediction.[97] Naturally, we attempt the same experiment for BZP by mixing 12.3 mol % of it with polystyrene having molecular weight of 800 (PS800). Representative spectra of BZP in the mixture at 153.15 and 163.15 K are presented in Figure 5 to show the presence of two secondary relaxations, in addition to the α-relaxation (not shown in the same figure). The relaxation times of the three processes observed in the mixture, denoted by $\hat{\tau}_\alpha$, τ_β, and τ_γ, at all measurement temperatures are plotted against reciprocal temperature and are shown in Figure 6. Included are the α-relaxation time, τ_α, and the secondary relaxation time, τ_{obs}, of neat BZP published in refs 44 and 45. Similar results for mixtures of BZP are reported also in an earlier work.[98] Considering the large uncertainties involved in determining τ_{obs} of neat BZP due to the large breadth of the observed secondary loss peak,[44,45] τ_γ of BZP in the mixture can be considered as nearly the same as τ_{obs}. This coincidence indicates that the faster secondary γ-relaxation of BZP observed in the mixture is the same as the only secondary relaxation found in neat BZP. The slower secondary relaxation observed in the mixture with relaxation time τ_β is thus the JG β-relaxation of BZP. These identifications demonstrate that the resolved secondary relaxation in neat BZP is not the JG β-relaxation of BZP because its relaxation time τ_{obs} is nearly the same as τ_γ in the mixture. As is evident by inspection of the Arrhenius plot (Figure 6), $\hat{\tau}_\alpha$ of BZP in the mixture is much longer than τ_α of neat BZP, while τ_γ remains nearly the same as τ_{obs}. This means a much wider separation between $\hat{\tau}_\alpha$ and τ_γ in the mixture than between τ_α and τ_{obs} in neat BZP and explains why the JG β-relaxation becomes resolved in the mixture. One way to further prove that the slower secondary relaxation in the mixture is the JG β-relaxation of BZP is by dielectric measurement at elevating pressure. If τ_β of BZP in the mixture shifts to longer times with increasing pressure like $\hat{\tau}_\alpha$, then this is further evidence of it being the relaxation time of the JG β-relaxation.

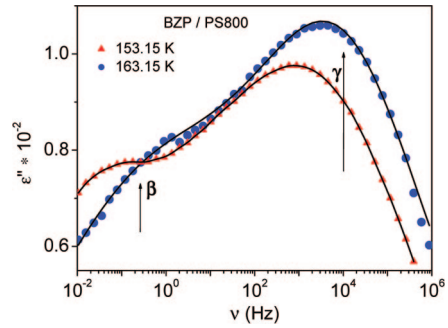

Figure 5. Dielectric loss spectra of 12.3% mole fraction BZP/PS800 mixture at 153.15 (triangles) and 163.15 K (circles) showing the presence of two secondary relaxations. Lines are the fit by the sum of two CC functions to the β- and γ-relaxations. The arrows mark the position of the maxima of the two processes at 163.15 K.

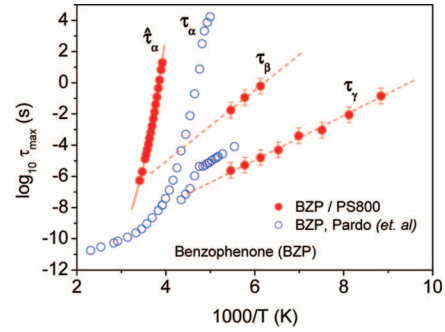

Figure 6. Arrhenius plot of the logarithm of relaxation time [$\tau_{max} = 1/(2\pi f_{max})$] vs $1000/T$ of 12.3% mole fraction BZP/PS800 mixture (filled circles) along the data of neat BZP from Pardo et al.[45] (open circles) for comparison. Solid and dashed lines are guides to the eye.

This pressure dependence was found before for picoline and QN in mixtures with tristyrene to confirm that the new secondary relaxation found in these mixtures is truly the JG β-relaxation of these molecules.[85,86] Preliminary dielectric measurements of the mixture of BZP with PS800 at elevated pressures have shown that τ_β of BZP shifts with pressure. The results will be reported elsewhere in the future.

DBP and its isomer, diisobutyl phthalate (DiBP), as well as other dialkly phthalates share the same problem as BZP in finding no evidence for the presence of the JG β-relaxation[99,100] in the dielectric spectra. A secondary relaxation was observed in all of these phthalates, but its relaxation time was shown to be pressure independent;[99,100] hence, it is not the JG β-relaxation.[51] This is a local and intramolecular relaxation involving likely the rotation of a part of the molecule (i.e., the alkyl chain) about the flexible oxygen bond. The dielectric loss spectra at ambient or elevated pressure show no features to indicate the presence of a slower secondary relaxation that can be identified as the JG β-relaxation. This situation again raises serious question on the validity of the claim of universality of the JG β-relaxation. A rationalization of this situation in the phthalates can be given like above for BZP because all dialkyl phthalates have narrow α-loss peaks and small coupling parameters n except dimethyl phthalate, which has the shortest alkyl side chain. For example, $n = 0.35$ for DBP and DiBP[99] and $n = 0.36$ for diethyl phthalate (DEP).[100] Like in the case of BZP, the expected $\nu_{JG} \approx \nu_0$ falls in between the high-frequency flank of the α-loss peak and the onset of the intense non-JG secondary relaxation; hence, the JG β-relaxation is not resolved. This rationalization cannot be convincing until the JG β-relaxation of the phthalates is made to appear by some method. Fortunately, the phthalates are polar molecules and the method of mixing with an apolar oligomer of styrene again can be used to detect their JG β-relaxation by dielectric spectroscopy. This task has recently been carried out successively in DMP, DEP, DBP, and DiBP. Here, we present representative dielectric loss data of 10% mol of DiBP mixture with PS800 to show the detection of two secondary relaxations in addition to the α-relaxation, all coming from motions of the DiBP molecules detected through their dipole moments. The faster secondary relaxation of DiBP in the mixture has the same relaxation times as the resolved non-JG secondary relaxation of neat DiBP, just as in the case of BZP. These results are shown in the Arrhenius plot of relaxation times of the two secondary relaxations and the α-relaxation observed in the mixture of DiBP with PS800 (Figure 7). Also shown are the relaxation times of the non-JG secondary relaxation and the α-relaxation of neat DiBP. By the same reasoning given before for BZP, the slower secondary relaxation in the mixture is the JG β-relaxation of DiBP that we are looking for. Mixtures of 10% mol of DMP or DEP with PS800 show exactly the same dynamics as seen in the mixture of DiBP with PS800. The slower secondary relaxation of DEP in the mixture appears prominently in the spectra, and this mixture is the best candidate to further check if it is the JG β-relaxation of DEP by performing dielectric measurements at elevated pressures. This has been done at the time of writing this paper, and in fact, the resolved JG β-relaxation shifts to lower frequencies significantly on increasing pressure. The data will be published elsewhere.

There are other methods showing the existence of the JG β-relaxation in all glass former besides introducing it as guest molecules in a host having higher T_g as described above. Isoeugenol (2-methoxy-4-propenyl phenol)[101] as well as another phthalate, dioctyl phthalate (DOP),[102] show no feature (not even an excess wing) in their isothermal dielectric spectra to indicate the presence of the JG β-relaxation, just like DEP, DBP, and DiBP studied here. On physical aging in the glassy state, a resolved peak and an excess wing show up in isoeugenol[101] and DOP,[102] respectively, to indicate the presence of the JG β-relaxation. For hydrogen-bonded systems, one method is to apply high pressure accompanied by higher temperatures. The treatment transforms the excess wing to a resolved JG β-relaxation. These are shown for di- and tripropylene glycols,[103] threitol,[104] and the monosaccharide, ribose.[105] The isothermal dielectric loss spectra of dipropyleneglycol dibenzoate (DPGDB) in every respect look similar to that of DBP and BZP, and also, the resolved secondary relaxation is the non-JG γ-relaxation.[106] However, the JG β-relaxation of DPGDB shows up on applying pressure and also by cooling into the glassy state.[106,107] Besides molecular and polymeric glass formers considered in this paper, JG β-relaxation has been found in carbohydrates, biopolymers, plastic crystals, metallic glasses, oxide glasses, and molten salts.[35] Hence, it is a ubiquitous dynamic process in all glass formers, although its detection by experiment may not be straightforward in all cases.

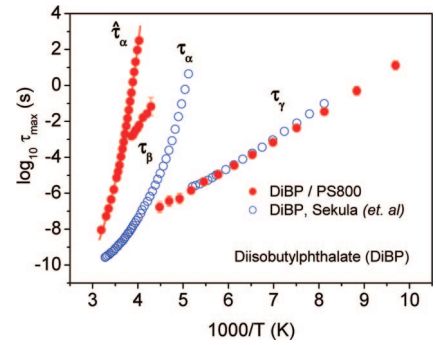

Figure 7. Arrhenius plot of the logarithm of relaxation time [$\tau_{max} = 1/(2\pi f_{max})$] vs $1000/T$ of the mixture, DiBP/PS800 (closed circles). The data of neat DiBP by Sekula et al.[99] (open circles) are also shown for comparison. The activation energy and the locations of the γ process of DiBP in the mixture and the neat state are nearly the same. A new slower β-process is present in the DiBP/PS800 mixture. The typical error bar for its relaxation time τ_β is indicated.

5. α-Relaxation

DBP, DiBP, DEP, and salol are glass formers among many more that the dynamics of the α-relaxation has been studied by dielectric spectroscopy at ambient pressure (0.1 MPa) as well as at elevated pressures up to 2 GPa in some cases. It was shown that the frequency dispersion of the entire α-loss peak of these glass formers is invariant to changes in the combinations of T and pressure P as long as τ_α is maintained constant.[35] Hence, the exponent $(1-n)$ of the KWW function (eq 2) that fits the shape of the α-loss peak is invariant to changes in the combinations of T and pressure P, while τ_α is maintained constant. This remarkable and general property of the α-relaxation is one indication of the fundamental importance of the frequency dispersion or the degree of nonexponentiality (measured by n) of the α-relaxation. It will be utilized later on in this section. Other indications of the width of the dispersion of the α-relaxation or its surrogate n either correlate or govern the properties of τ_α can be found in refs 35, 84, 108, and 109.

Although the dielectric relaxation data of the resolved secondary relaxation of neat BZP do not support the explanation of the IPL with $c \ll 1$ by the CC relaxation predicted by the latest version of MCT with RT coupling included, there are other features of the α-relaxation of BZP that were compared

favorably with the predictions of the idealized MCT.[44] One prediction is the critical law, $\tau_\alpha \propto (T - T_c)^{-\gamma}$ for $T > T_c$. Good agreement with experimental data was reported with values of $T_c = 250$ K and $\gamma = 1.92$. However, this critical law cannot describe the T dependence of τ_α below the putative $T_c = 250$ K and τ_α longer than about 10^{-8} s. A single Vogel−Fulcher−Tammann−Hesse (VFTH) equation does not fit the data well over any extended range of the entire range $10^{-11} < \tau_\alpha < 10^3$ s. This situation can be recognized from the scatter of the data about the fit shown in Figure 2 of ref 44. Actually, at temperatures higher than about 300 K, an Arrhenius law, $\tau_\alpha \propto \tau_\infty \exp(E_a/RT)$, with $E_a \approx 5$ kcal/mol, fits the T dependence of τ_α equally well as the fit by the MCT critical law over the same temperature range. This Arrhenius T dependence of τ_α or viscosity η at temperatures high above T_g was found before in many small molecular glass formers[110−116] including the classical case of 1,3-bis(1-naphthyl)-5-(2-naphthyl)benzene (TNB).[110] The activation enthalpy $E_a \approx 5$ kcal/mol of BZP is about the same as that of OTP.[117] In the other glass formers, the Arrhenius T dependence of τ_α or η fails at lower temperatures and two VFTH laws in separate temperature ranges are needed for a quantitative description of the data throughout the equilibrium liquid state.[110,113−116] An objective method to see the change of T dependence of x ($=\tau_\alpha$ or η) is to examine the dependence of $S(1/T) \equiv [\mathrm{d}\log x/\mathrm{d}(1/T)]^{-1/2}$ on $1/T$, a method introduced by Stickel.[113] A VFTH dependence of x, $A\exp[D/(T - T_0)]$, corresponds to $S(1/T) = (D/2.303)^{-1/2}[1 - (T_0/T)]$, and the latter shows up as a straight line in a plot of $S(1/T)$ against $1/T$. The requirement of two different VFTH laws to fit the data is then clear when two linear dependences with different slopes appear in the plot of $S(1/T)$ against $1/T$. The temperature that separates the two VFTH dependences was called T_B. If x has Arrhenius temperature dependence, $x_\infty \exp(E_a/RT)$, at high temperatures, the corresponding $S(1/T)$ is a constant independent of $1/T$ given by $(E_a/2.303R)^{-1/2}$. In a plot against $1/T$, the change of $S(1/T)$ from a constant to a linear dependence indicates the crossover from Arrhenius law to the VFTH law. The temperature at which the crossover occurs was called T_A, and invariably $T_A > T_B$. When finely spaced data of x over a wide range of temperature are available like in many glass formers,[110,113,114] the well-defined $S(1/T)$ show the aforesaid changes of T dependence of x at T_A and T_B. The data of τ_α of BZP obtained so far from dielectric measurements[44] are not as finely spaced as desired. Nevertheless, $S(1/T)$ calculated from the data[118] show evidence of crossover with decreasing temperature from Arrhenius law at high temperatures to the first VFTH law at $T_A \approx 350$ K and crossover from the first VFTH law to the second VFTH law at $T_B \approx 240$ K and $\tau_\alpha(T_B) = 10^{-6.2}$ s. The overall temperature dependence of BZP is therefore qualitatively the same as the other glass formers. Let us compare $\tau_\alpha(T_B)$ of BZP with those of other glass formers. At $T = T_B$, PDE and propanol[114] have the longest relaxation times with $\tau_\alpha(T_B) = 10^{-3.6}$ and $10^{-3.7}$ s, respectively, and polychlorinated biphenol (PCB62) has $\tau_\alpha(T_B) = 10^{-5.9}$ s. BMMPC has $\tau_\alpha(T_B) = 10^{-6.1}$ s. KDE and salol has $\tau_\alpha(T_B) = 10^{-6.3}$ s. PC has $\tau_\alpha(T_B) = 10^{-7.0}$ s,[115] and the much studied epoxy resin, diglycidyl ether of bisphenol-A (DGEBA), has $T_B = 275$ K and $\tau_\alpha(T_B) = 10^{-4.3}$ s.[116] From these results, it is clear that $\tau_\alpha(T_B)$ varies over a wide range (more than 6 orders of magnitude from $10^{-3.6}$ to $10^{-10.3}$ s) when all glass formers are considered. Hence, the results invalidate the claim that $\tau_\alpha(T_B)$ has "universal" or "magic" value lying within the narrow range of $10^{-6.5}$−$10^{-7.5}$ s.[119] Connection was made of the crossover temperature T_B to the critical temperature T_c of MCT.[119] This proposal is also refuted by the fact that PDE and DGEBA have $\tau_\alpha(T_B) = 10^{-3.6}$ s and $\tau_\alpha(T_B) = 10^{-4.3}$ s, respectively, because it is inconceivable that such a long or macroscopic relaxation time can be associated with T_c of MCT.

Keen observation was made[120,121] of the presence of correlation between the crossover of T-dependence of τ_α at T_A and T_B with the corresponding change of the size and T dependence of the width of the dispersion of the α-loss peak, or equivalently the size of n appearing in the exponent $(1 - n)$ of the KWW function (eq 2) or the exponent β_{CD} of the Cole−Davidson function that fits it.[44] For the same α-loss peak, n is slightly less than $(1 - \beta_{CD})$. From broadband dielectric relaxation data of many small molecular glass formers, it was shown that n is close to zero or β_{CD} slightly less than 1 in the high temperature regime of $T > T_A$ where τ_α has Arrhenius dependence. Noticeable monotonic increase of n from near zero (or decrease of β_{CD} from near 1) with decreasing temperature starts after crossing T_A. This behavior of β_{CD} is indeed found in BZP across its $T_A \approx 350$ K (see Figure 4 of ref 44). There is yet another change of temperature dependence of n (or β_{CD}) when crossing T_B. This is also found in BZP when crossing its $T_B \approx 240$ K (see Figure 4 of ref 44). The change of the size and T dependence of n shadowing the change of T dependence of τ_α when crossing T_B is the basis of the explanation of the latter by the CM.[122] This explanation can be qualitatively understood from eq 3 by the dependence of τ_α on both n and τ_0. The abrupt change of T dependence of n across T_B necessarily introduces two different VFTH laws for $\tau_\alpha(P_B)$ even though a single VFTH law describes the T dependence of τ_0 for all the temperatures. This effect has been demonstrated using dielectric relaxation data of several glass formers in ref 122. Support of this explanation comes from the experimental observation of the crossover phenomenon at elevated pressures P. The crossover from one VFTH law to another found at ambient pressure was also found at elevated pressure, albeit T_B is a function of P and increases with P. Remarkably, the α-relaxation time $\tau_\alpha[T_B(P)]$ is a constant independent of P and $T_B(P)$, although the density and entropy of the glass formers vary over large ranges with different combinations of P and $T_B(P)$ in these experiments.[115] These experimental results demonstrate that the crossover phenomenon at $T_B(P)$ arises not at some critical temperature or density; rather, we have the same $\tau_\alpha[T_B(P)]$ at $T_B(P)$ for any pressure, therefore, the same value of $n[T_B(P)]$. The last deduction follows from the coinvariance of τ_α and n to different combinations of P and T discussed at the beginning of this section found for many glass formers including the ones considered here.[35,85,86] The explanation of the change of the T dependence of τ_α across T_B by change of T dependence of n across T_B given for ambient pressure applies verbatim at any elevated pressure.

The α-relaxation strength, $\Delta\varepsilon_\alpha$, of BZP obtained as a function of temperature from fits of the data by the Cole−Davidson function show a bump in a neighborhood of temperature around 240 K, which is T_c and also T_B of BZP.[44] The product, $T\Delta\varepsilon_\alpha$, was shown to exhibit a cusp anomaly near 240 K like that predicted by the idealized MCT for the nonergodicity parameter at T_c. This product $T\Delta\varepsilon_\alpha$ also was considered in earlier works for various glass formers including DBP, salol, propylene carbonate, glycerol, and propylene glycol,[112] but there either no cusp at T_c or pseudocusp with the wrong shape was observed, and disagreements with MCT predictions were noted. Thus, the MCT-like cusp of $T\Delta\varepsilon_\alpha$ found in BZP is an exception, possibly caused by the mode of change of n at T_B in BZP is unlike that of other glass formers. For this reason and others, we consider

an alternative explanation of the anomaly of $\Delta\varepsilon_\alpha$ from consideration of T_B in the following paragraph.

As mentioned above, a similar anomaly of $\Delta\varepsilon_\alpha$ at T_B was found before in other glass formers including DBP and salol.[112,123] The change of the temperature dependence of the dynamics causing the crossover of the T dependence of τ_α from $(VFTH)_1$ to $(VFTH)_2$ at T_B is expected to have an effect of the relaxation strength. This is because both the relaxation strength and the relaxation time τ_α are complimentary characteristics of the dynamics. Concomitant changes of τ_α and $\Delta\varepsilon_\alpha$ were best shown[123] in a plot of $\Delta\varepsilon_\alpha$ against $\log\nu_\alpha$ for DBP, salol, and propylene carbonate, where ν_α is the α-loss peak frequency and is approximately the same as $1/(2\pi\tau_\alpha)$. These plots indicate two different dependences of $\Delta\varepsilon_\alpha$ on $\log\nu_\alpha$, which when extrapolated intersect at a crossover frequency ν_B. It turns out that for all the glass formers, ν_B is nearly the same as $1/[2\pi\tau_\alpha(T_B)]$. Similar results were found also for the polymer, poly(vinylacetate)[124,125] and most recently in an amorphous pharmaceutical, ibuprofen.[126] Therefore, the change of the dependence of $\Delta\varepsilon_\alpha$ on $\log\nu_\alpha$ also occurs at the temperature T_B. This phenomenon can also be explained by the more rapid increase of n with decreasing temperature (frequency) after crossing T_B (ν_B), because n reflects the nonexponentiality and the extent or length-scale of the cooperative many-body α-relaxation and, in turn, the magnitude of $\Delta\varepsilon_\alpha$. The temperature dependence of $\Delta\varepsilon_\alpha$ is roughly proportional to $1/T$ at temperature much higher than T_B consistent with the Kirkwood−Fröhlich theory based on the assumption of noninteracting isolated dipoles as reflected by the smaller values of n therein. However, this dependence of $\Delta\varepsilon_\alpha$ does not continue when temperature is lowered to approach T_B and below T_B because n increases significantly on further decrease in temperature. Thus, the observed anomaly of the T dependence of $\Delta\varepsilon_\alpha$ in a neighborhood of T_B is another consequence of the change of the temperature dependence of n or the degree of cooperativity of the α-relaxation with falling temperature after crossing T_B.[120,121] The detail of the change of n in crossing T_B in BZP is different from the other glass formers including salol, DBP, propylene carbonate, and propylene glycol. In BZP, n or $(1-\beta_{CD})$ increases on approaching T_B with falling temperature from above to reach a value at T_B and maintains approximately this value when falling below T_B (see Figure 4 in ref 44). On the other hand, in the other glass formers, n is slowly varying and small when $T > T_B$ and rapidly increases with decreasing temperature after crossing T_B.[120,121] This difference in the change of temperature dependence of n when crossing T_B of BZP from the other glass formers may explain the cusp anomaly of $T\Delta\varepsilon_\alpha$ found in BZP but not in the others.

6. Conclusion

Relaxation and diffusion in complex and interacting systems including glass formers differ from other research fields in various ways. The differences include the diversity of the physical and chemical structures of the systems or substances investigated, the wide range of phenomena exemplified, the variety of dynamics transpiring from picoseconds to days, the large volume of experimental data indicating general and important properties, the intriguing manner in which one dynamic process evolves with time, and the existence of relation with the dynamic process that follows in time. It is not possible to fully solve the problem without taking into consideration all of the processes, the general properties of each individual process, and the connections between them. Thus, in the research field of glass transition, experimental facts and phenomenology are indispensable guides in the construction of viable theory. In the opposite way, theory coming out solely from a theoretical basis, no matter how mathematically rigorous but not aware of the full spectrum of important experimental facts, is unlikely to be able to explain the rich properties of the various dynamic processes and their inter-relationship. This point of view is supported in this paper by the discussion of experimental data and theory of three ubiquitous and interconnected dynamic processes: the caged dynamics, the JG β-relaxation, and the α-relaxation. The remarkable properties of each individual process and their inter-relations demonstrate the need of considering all three processes and putting emphasis on experimental facts. Fixation on any theory, no matter how rigorous but not having addressed all three processes to fully reconcile with the experimental facts, is not the way to make significant progress.

Acknowledgment. The work at the Università di Pisa was supported by MIUR-FIRB 2003 D.D.2186 grant RBNE03R78E. M.S.T. kindly acknowledges the support from MIUR ("Borse a Favore di Giovani Ricercatori Indiani", no. 1451, 28/07/2005"). K.L.N. was supported by the Office of Naval Research and a travel grant for International Semester Exchange Collaboration provided by the International Materials Institute for New Functionality in Glass, Lehigh University, funded by NSF.

References and Notes

(1) Bengtzelius, U.; Götze, W.; Sjölander, A. *J. Phys. C* **1984**, *17*, 5915. Leutheuser, E. *Phys. Rev. A* **1984**, *29*, 2765.
(2) Götze, W.; Sjögren, L. *Rep. Prog. Phys.* **1992**, *55*, 241.
(3) Götze, W. *Liquids, Freezing, and the Glass Transition*; Les Houches Lectures; North-Holland: Amsterdam, 1991; p 289.
(4) Götze, W. *J. Phys.: Condens. Matter* **1999**, *11*, A1.
(5) Sjögren, L. *Phys. Rev. A* **1986**, *33*, 1254.
(6) Fuchs, M.; Götze, W.; Hildebrand, S.; Latz, A. *J. Phys.: Condens. Matter* **1992**, *4*, 7709.
(7) Cummins, H. Z.; Du, W. M.; Fuchs, M.; Götze, W.; Hildebrand, S.; Latz, A.; Li, G.; Tao, N. J. *Phys. Rev. E* **1993**, *47*, 4223.
(8) Du, W. M.; Li, G.; Cummins, H. Z.; Fuchs, M.; Toulouse, J.; Knauss, L. A. *Phys. Rev. E* **1994**, *49*, 2192.
(9) Götze, W.; Sperl, M. *Phys. Rev. E* **2002**, *66*, 011405.
(10) Götze, W.; Sperl, M. *Phys. Rev. Lett.* **2004**, *92*, 105701.
(11) Sperl, M. *Phys. Rev. E* **2006**, *74*, 011503.
(12) Lebon, M. J.; Dreyfus, C.; Li, G.; Aouadi, A.; Cummins, H. Z.; Pick, R. M. *Phys. Rev. E* **1995**, *51*, 4537.
(13) Engberg, D.; Wischnewski, A.; Buchenau, U.; Börjesson, L.; Dianoux, A. J.; Sokolov, A. P.; Torell, L. M. *Phys. Rev. B* **1998**, *58*, 9087.
(14) Hinze, G.; Brace, D. D.; Gottke, S. D.; Fayer, M. D. *J. Chem. Phys.* **2000**, *113*, 3723.
(15) Cang, H.; Novikov, V. N.; Fayer, M. D. *J. Chem. Phys.* **2003**, *118*, 2800.
(16) Bartsch, E.; Antonietti, M.; Schupp, W.; Sillescu, H. *J. Chem. Phys.* **1992**, *97*, 3950.
(17) Smith, N. A.; Meech, S. R. *Int. Rev. Phys. Chem.* **2002**, *21*, 75.
(18) Sokolov, A. P.; Kisliuk, A.; Novikov, V. N.; Ngai, K. L. *Phys. Rev. B* **2001**, *63*, 172204.
(19) Brodin, A.; Rössler, E. A. *J. Chem. Phys.* **2006**, *125*, 114502.
(20) Sokolov, A. P. Unpublished data.
(21) Ngai, K. L. *Philos. Mag.* **2004**, *84*, 1341.
(22) Kisliuk, A.; Novikov, V. N.; Sokolov, A. P. *J. Polym. Sci., Part B: Polym. Phys.* **2002**, *40*, 201–209.
(23) Lunkenheimer, P.; Schneider, U.; Brand, R.; Loidl, A. *Contemp. Phys.* **2000**, *41*, 15.
(24) Brodin, A.; Gainaru, C.; Porokhonsky, V.; Rössler, E. A. *J. Phys.: Condens. Matter* **2007**, *20*, 205104.
(25) Blochowicz, T.; Tschirwitz, C.; Benkhof, S.; Rössler, E. A. *J. Chem. Phys.* **2003**, *118*, 7544.
(26) Blochowicz, T.; Gainaru, C.; Medick, P.; Tschirwitz, C.; Rössler, E. A. *J. Chem. Phys.* **2006**, *124*, 134503.
(27) Brodin, A.; Rössler, E. A. *J. Chem. Phys.* **2007**, *126*, 244508.
(28) Ngai, K. L.; Léon, C. *Phys. Rev. B* **2002**, *66*, 064308. (b) Data taken from Lunkenheimer, P.; Pimenov, A.; Loidl, A. *Phys. Rev. Lett.* **1997**, *78*, 2995. (c) Lunkenheimer, P. *Dielectric Spectroscopy of Glassy Dynamics*; Aachen: Shaker, 1999.

(29) Howell, F. S.; Bose, R. A.; Macedo, P. B.; Moynihan, C. T. *J. Phys. Chem.* **1974**, *78*, 639.

(30) Hofmann, A.; Kremer, F.; Fischer, E. W.; Schönhals, A. In *Disorder Effects on Relaxational Processes*; Richert, R., Blumen, A., Eds.; Springer: Berlin, 1994; p 309.

(31) Kudlik, A.; Benkhof, S.; Blochowicz, T.; Tschirwitz, C.; Rössler, E. A. *J. Mol. Struct.* **1999**, *479*, 201.

(32) Data of N-methyl-ε-caprolactam (NMEC) were made available to us by R. Richert.

(33) Ngai, K. L.; Lunkenheimer, P.; Léon, C.; Schneider, U.; Brand, R.; Loidl, A. *J. Chem. Phys.* **2001**, *115*, 1405.

(34) Ngai, K. L. *J. Chem. Phys.* **1998**, *109*, 6982.

(35) Ngai, K. L.; Casalini, R.; Capaccioli, S.; Paluch, M.; Roland, C. M. *J. Phys. Chem. B* **2005**, *109*, 17356. Ngai, K. L.; Casalini, R.; Capaccioli, S.; Paluch, M.; Roland, C. M. *Adv. Chem. Phys. Part B, Fractals Diffusion Relaxation in Disordered Complex Systems*; Kalmykov, Y. P., Coffey, W. T., and Rice, S. A., Eds.; J. Wiley and Sons: New York, 2006; Vol. 133, Chapter 10, p 497.

(36) (a) Ngai, K. L.; Capaccioli, S. *J. Phys.: Condens. Matter* **2008**, *20*, 244101. (b) Ngai, K. L.; Prevosto, D.; Capaccioli, S.; Roland, C. M. *J. Phys.: Condens. Matter* **2008**, *20*, 244125.

(37) Böhmer, R.; Diezemann, G.; Geil, B.; Hinze, G.; Nowaczyk, A.; Winterlich, M. *Phys. Rev. Lett.* **2006**, *97*, 135701.

(38) Nowaczyk, A.; Geil, B.; Hinze, G.; Böhmer, R. *Phys. Rev. E* **2006**, *74*, 041505.

(39) Roland, C. M.; Schroder, M. J.; Fontanella, J. J.; Ngai, K. L. *Macromolecules* **2004**, *37*, 2630.

(40) Slaytona, R. M.; Nelson, K. A. *J. Chem. Phys.* **2004**, *120*, 3919.

(41) Gottke, S. D.; Brace, D. D.; Hinze, G.; Fayer, M. D. *J. Phys. Chem. B* **2001**, *105*, 238.

(42) Brace, D. D.; Gottke, S. D.; Cang, H.; Fayer, M. D. *J. Chem. Phys.* **2002**, *116*, 1598.

(43) Cole, K. S.; Cole, R. H. *J. Chem. Phys.* **1941**, *9*, 341.

(44) Lunkenheimer, P.; Pardo, L. C.; Kohler, M.; Loidl, A. *Phys. Rev. E* **2008**, *77*, 031506.

(45) Pardo, L. C.; Lunkenheimer, P.; Loidl, A. *Phys. Rev. E* **2007**, *76*, 030502(R)

(46) (a) Murata, K.; Hanawa, A.; Nozaki, R. *J. Appl. Phys.* **2005**, *98*, 084107. (b) Nozaki, R. To be published. (c) Döss, A.; Paluch, M.; Sillescu, H.; Hinze, G. *J. Chem. Phys.* **2002**, *117*, 6582. (d) Kubo, E.; Minoguchi, A.; Sotokawa, H.; Nozaki, R. *J. Non-Cryst. Solids* **2006**, *352*, 4724.

(47) Caliskan, G.; Kisliuk, A.; Novikov, V. N.; Sokolov, A. P. *J. Chem. Phys.* **2001**, *114*, 10189.

(48) Adichtchev, S.; Blochowicz, T.; Gainaru, C.; Novikov, V. N.; Rössler, E. A.; Tschirwitz, C. *J. Phys.: Condens. Matter* **2003**, *15*, S835.

(49) Ngai, K. L. *J. Phys.: Condens. Matter* **2003**, *15*, S1107.

(50) Ngai, K. L.; Paluch, M. *J. Phys. Chem. B* **2003**, *107*, 6865.

(51) Ngai, K. L.; Paluch, M. *J. Chem. Phys.* **2004**, *120*, 857.

(52) Ngai, K. L.; Casalini, R. *Phys. Rev. B* **2002**, *66*, 132205.

(53) Rösner, P.; Samwer, K.; Lunkenheimer, P. *Eur. Phys. Lett.* **2004**, *68*, 226.

(54) Hachenberg, J.; Samwer, K. *J. Non-Cryst. Solids* **2006**, *352*, 5110.

(55) Ngai, K. L. *J. Non-Cryst. Solids* **2006**, *352*, 404.

(56) Cummins, H. Z. *J. Phys.: Condens. Matter* **2005**, *17*, 1457.

(57) Petry, W.; Bartsch, E.; Fujara, F.; Kiebel, M.; Sillescu, H.; Farago, B. *Z. Phys. B* **1991**, *83*, 175.

(58) Kiebel, M.; Bartsch, E.; Debus, O.; Fujara, F.; Sillescu, H. *Phys. Rev. B* **1992**, *45*, 10301.

(59) Wuttke, J.; Kiebel, M.; Bartsch, E.; Fujara, F.; Petry, W.; Sillescu, H. *Z. Phys. B* **1993**, *91*, 357.

(60) Tölle, A.; Schober, H.; Wuttke, J.; Fujara, F. *Phys. Rev. E* **1997**, *56*, 809.

(61) Li, G.; Du, M.; Sakai, A.; Cummins, H. Z. *Phys. Rev. A* **1992**, *46*, 3343.

(62) Li, G.; Du, W. M.; Chen, X. K.; Cummins, H. Z.; Tao, N. Z. *Phys. Rev. A* **1992**, *45*, 3867.

(63) Cummins, H. Z.; Hwang, Y. H.; Li, G.; Du, W. M.; Losert, W.; Shen, G. Q. *J. Non-Cryst. Solids* **1998**, *235*−*237*, 254.

(64) Data of Mezei, F. *J. Non-Cryst. Solids* **1991**, *131*−*133*, 317 as interpreted by Cummins, H. Z.; Du, W. M.; Fuchs, M.; Gotze, W.; Hildebrand, S.; Latz, A.; Li, G.; Tao, N. J. *Phys. Rev. E* **1993**, *47*, 4223.

(65) Pimenov, A.; Lunkenheimer, P.; Rall, H.; Kohlhaas, R.; Loidl, A.; Böhmer, R. *Phys. Rev. E* **1996**, *54*, 676.

(66) Lunkenheimer, P.; Pimenov, A.; Loidl, A. *Phys. Rev. Lett.* **1997**, *78*, 2995.

(67) Lunkenheimer, P. *Dielectric Spectroscopy of Glassy Dynamics*; Shaker: Aachen, 1999.

(68) Mezei, F.; Knaak, W.; Farago, B. *Phys. Rev. Lett.* **1987**, *58*, 571.

(69) Ngai, K. L.; León, C. *Phys. Rev. B* **2002**, *66*, 064308.

(70) Ngai, K. L.; Habasaki, J.; Hiwatari, Y.; León, C. *J. Phys.: Condens. Matter* **2003**, *15*, S1607. Habasaki, J.; Ngai, K. L. *J. Non-Cryst. Solids* **2006**, *352*, 5170.

(71) Courtland, R. E.; Weeks, E. R. *J. Phys.: Condens. Matter* **2003**, *15*, S359.

(72) Ngai, K. L. *Philos. Mag.* **2007**, *87*, 357.

(73) León, C.; Rivera, A.; Várez, A.; Sanz, J.; Santamaria, J.; Ngai, K. L. *Phys. Rev. Lett.* **2001**, *86*, 1279.

(74) Weeks, E. R.; Weitz, D. A. *Phys. Rev. Lett.* **2002**, *89*, 095704.

(75) Ngai, K. L.; Rendell, R. W.; León, C. *J. Non-Cryst. Solids* **2002**, *307*−*310*, 1039.

(76) Johari, G. P.; Goldstein, M. *J. Chem. Phys.* **1970**, *53*, 2372.

(77) Johari, G. P. *Ann. N. Y. Acad. Sci.* **1976**, *279*, 117.

(78) Capaccioli, S.; Prevosto, D.; Kessairi, K.; Lucchesi, M.; Rolla, P. A. *J. Non-Cryst. Solids* **2007**, *353*, 3984.

(79) Nath, R.; Nowaczyk, A.; Geil, B.; Böhmer, R. *J. Non-Cryst. Solids* **2007**, *353*, 3788.

(80) Nogales; Sanz, A.; Ezquerra, T. A. *J. Non-Cryst. Solids* **2006**, *352*, 4649.

(81) Brand, R.; Lunkenheimer, P.; Loidl, A. *J. Chem. Phys.* **2002**, *116*, 10386.

(82) Ngai, K. L. *Comment. Solid State Phys.* **1979**, *9*, 141.

(83) Ngai, K. L.; Tsang, K. Y. *Phys. Rev. E* **1999**, *60*, 4511. Tsang, K. Y.; Ngai, K. L. *Phys. Rev. E* **1996**, *54*, R3067. Ngai, K. L.; Peng, S. L.; Tsang, K. Y. *Phys. A* **1992**, *191*, 523. (d) Tsang, K. Y.; Ngai, K. L. *Phys. Rev. E* **1997**, *56*, R17.

(84) Ngai, K. L. *IEEE Trans. Dielectr. Electr. Insul.* **2001**, *8*, 329.

(85) Mierzwa, M.; Pawlus, S.; Paluch, M.; Kaminska, E.; Ngai, K. L. *J. Chem. Phys.* **2008**, *128*, 044512.

(86) Kessairi, K.; Capaccioli, S.; Prevosto, D.; Lucchesi, M.; Sharifi, S.; Rolla, P. A. *J. Phys. Chem. B* **2008**, *112*, 4470.

(87) Diezemann, G.; Mohanty, U.; Oppenheim, I. *Phys. Rev. E* **1999**, *59*, 2067.

(88) Zhao, Z. F.; Wen, P.; Shek, C. H.; Wang, W. H. *Phys. Rev. B* **2007**, *75*, 174201.

(89) Pelletier, J. M.; Van de Moortele, B.; Lu, I. R. *Mater. Sci. Eng., A* **2002**, *336*, 190.

(90) Leslie-Pelecky, D. L.; Birge, N. O. *Phys. Rev. Lett.* **1994**, *72*, 1232.

(91) Greenall, M. J.; Cates, M. E. *Phys. Rev. E* **2007**, *75*, 051503.

(92) Ngai, K. L.; Lunkenheimer, P.; Leon, C.; Schneider, U.; Brand, R.; Loidl, A. *J. Chem. Phys.* **2001**, *115*, 1405.

(93) Capaccioli, S.; Ngai, K. L. *Phys.Chem. B* **2005**, *109*, 9727.

(94) Blochowicz, T.; Rössler, E. A. *Phys. Rev. Lett.* **2004**, *92*, 225701.

(95) Capaccioli, S.; Kessairi, K.; Prevosto, D.; Lucchesi, M.; Rolla, P. A. *J. Phys.: Condens. Matter* **2007**, *19*, 205133.

(96) Bedrov, D.; Smith, G. D. *Macromolecules* **2005**, *38*, 10314. Bedrov, D.; Smith, G. D. *Macromolecules* **2006**, *39*, 8526.

(97) Ngai, K. L.; Capaccioli, S.; Roland, C. M. *Macromolecules* **2006**, *39*, 8543.

(98) Desando, M. A.; Gourlay, D. L.; Walker, S. *J. Chem. Soc. Faraday Trans. 2* **1983**, *79*, 559.

(99) Sekula, M.; Pawlus, S.; Hensel-Bielowka, S.; Ziolo, J.; Paluch, M.; Roland, C. M. *J. Phys. Chem. B* **2004**, *108*, 4997.

(100) Pawlus, S.; Paluch, M.; Sekula, M.; Ngai, K. L.; Rzoska, S. J.; Ziolo, J. *Phys. Rev. E* **2003**, *68*, 021503.

(101) Kaminska, E.; Kaminski, K.; Paluch, M.; Ngai, K. L. *J. Chem. Phys.* **2006**, *124*, 164511.

(102) Kaminska, E.; Kaminski, K.; Hensel-Bielowka, S.; Paluch, M.; Ngai, K. L. *J. Non-Cryst. Solids* **2006**, *352*, 4672.

(103) Casalini, R.; Roland, C. M. *Phys. Rev. B,* **2004**, *69*, 094202.

(104) Hensel-Bielowka, S.; Pawlus, S.; Roland, C. M.; Zioło, J.; Paluch, M. *Phys. Rev. E* **2004**, *69*, 050501.

(105) Kaminska, K.; Kaminski, E.; Ziolo, J.; Paluch, M.; Ngai, K. L. *J. Phys. Chem. B* **2006**, *110*, 25045.

(106) Prevosto, D.; Capaccioli, S.; Lucchesi, M.; Rolla, P. A.; Ngai, K. L. *J. Chem. Phys.* **2004**, *120*, 4808.

(107) Capaccioli, S.; Prevosto, D.; Lucchesi, M.; Rolla, P. A.; Casalini, R.; Ngai, K. L. *J. Non-Cryst. Solids* **2005**, *351*, 2643.

(108) Ngai, K. L. *J. Non-Cryst. Solids* **2000**, *275*, 7.

(109) Ngai, K. L.; Capaccioli, S. *J. Phys.: Condens. Matter* **2007**, *19*, 205114.

(110) (a) Plazek, D. J.; Magill, J. H. *J. Chem. Phys.* **1968**, *49*, 3678. (b) Ngai, K. L.; Magill, J. H.; Plazek, D. J. *J. Chem. Phys.* **2000**, *112*, 1887.

(111) Schönhals, A.; Kremer, F.; Schlosser, E. *Phys. Rev. Lett.* **1991**, *67*, 999.

(112) Schönhals, A.; Kremer, F.; Hofmann, A.; Fischer, E. W.; Schlosser, E. *Phys. Rev. Lett.* **1993**, *70*, 3459.

(113) Stickel, F. Ph.D. Dissertation, Univ. Mainz, 1995 (Shaker, Aachen). Stickel, F.; Fischer, E. W.; Richert, R. *J. Chem. Phys.* **1995**, *102*, 6251. Stickel, F.; Fischer, E. W.; Richert, R. *J. Chem. Phys.* **1996**, *104*, 2043.

(114) Hansen, C.; Stickel, F.; Richert, R.; Fischer, E. W. *J. Chem. Phys.* **1997**, *107*, 1086.

(115) Casalini, R.; Paluch, M.; Roland, C. M. *J. Chem. Phys.* **2003**, *118*, 5701. Casalini, R.; Paluch, M.; Roland, C. M. *J. Phys.: Condens. Matter* **2003**, *15*, S859. Casalini, R.; Roland, C. M. *Phys. Rev. B* **2005**, *71*, 014210.

(116) Corezzi, S.; Beiner, M.; Huth, H.; Schröter, K.; Capaccioli, S.; Casalini, R.; Fioretto, D.; Donth, E. *J. Chem. Phys.* **2002**, *117*, 2435.

(117) Ngai, K. L.; Habasaki, J.; León, C.; Rivera, A. *Z. Phys. Chem.* **2005**, *219*, 47.

(118) Lunkenheimer, P. Private communication, 2008.

(119) Novikov, V. N.; Sokolov, A. P. *Phys. Rev. E* **2003**, *67*, 031507.

(120) León, C.; Ngai, K. L. *J. Phys. Chem. B* **1999**, *103*, 4045.

(121) Ngai, K. L. *J. Chem. Phys.* **1999**, *111*, 3639.

(122) Casalini, R.; Ngai, K. L.; Roland, C. M. *Phys. Rev. B* **2003**, *68*, 014201.

(123) Schönhals, A. *Europhys. Lett.* **2001**, *56*, 815.

(124) Ngai, K. L.; Roland, C. M. *Polymer* **2002**, *43*, 567.

(125) Tyagi, M.; Alegría, A.; Colmenero, J. *J. Chem. Phys.* **2005**, *122*, 244909.

(126) Brás, A. R.; Noronha, J. P.; Antunes, A. M. M.; Cardoso, M. M.; Schönhals, A.; Affouard, F.; Dionísio, M.; Correia, N. T. *J. Phys. Chem. B* **2008**, *112*, 11087.

JP8057433